Surface Modification of SU-8 Based Nanopore Arrays to Enhance Intracortical Brain-Machine Interface

Eunhee Kim(김 은 희 金 銀 姬)

Department of Robotics Engineering

로봇공학전공

DGIST

2013

Surface Modification of SU-8 Based Nanopore Arrays to Enhance Intracortical Brain-Machine Interface

Eunhee Kim(김 은 희 金 銀 姬)

Department of Robotics Engineering

로봇공학전공

DGIST

2013

Surface Modification of SU-8 Based Nanopore Arrays to Enhance Intracortical Brain-Machine Interface

Advisor   :   Professor   Hongsoo Choi

Co-advisor :   Professor   Jae-Eun Jang

by

Eunhee Kim

Department of Robotics Engineering

DGIST

A thesis submitted to the faculty of DGIST in partial fulfillment of the requirements for the degree of Master of Science in the Department of Robotics Engineering. The study was conducted in accordance with Code of Research Ethics[1].

07. 10. 2013

Approved by

Professor   Hongsoo Choi   (Signature)
(Advisor)

Professor   Jae-Eun Jang   (Signature)
(Co-Advisor)

---

[1] Declaration of Ethical Conduct in Research: I, as a graduate student of DGIST, hereby declare that I have not committed any acts that may damage the credibility of my research. These include, but are not limited to: falsification, thesis written by someone else, distortion of research findings or plagiarism. I affirm that my thesis contains honest conclusions based on my own careful research under the guidance of my thesis advisor.

Surface Modification of SU-8 Based Nanopore Arrays to Enhance Intracortical Brain-Machine Interface

Eunhee Kim

Accepted in partial fulfillment of the requirements for the degree of Master of Science.

06. 07. 2013

Head of Committee_____최 홍 수_____ (인)

Prof. Hongsoo Choi

Committee Member_____장 재 은_____ (인)

Prof. Jae-Eun Jang

Committee Member_____유 성 운_____ (인)

Prof. Seong-Woon Yu

Abstract

Over the past few years, several studies have been made on microelectrodes for invasive Brain-Machine Interface (BMI). In this field, one of the main issues is the formation of glia scar that acts as insulating layer on the surface of the implanted microelectrodes. Therefore, it is essential to modify the surface of the microelectrodes to enhance the life time of the microelectrodes.

In this study, the effect of nanoporous topography on SU-8 surface was investigated for neurite development using PC12 (neuron like cell) cells. Well-organized nanoporous SU-8 surface was fabricated using nanosphere lithography (NSL) by means of polystyrene nanoparticles. The diameter of nanopores was approximately 200 nm. Its size is similar to the size of filopodia. Cells were cultured on SU-8 surfaces with four different conditions: smooth bare surface, smooth bare surface coated with poly-L-lysine (PLL), nanoporous surface and nanoporous surface coated with PLL. The objective of this study is investigation of the neurite development on the four different surfaces.

The results of differentiation level showed cells were nearly not differentiated on smooth surface. However, PLL coated smooth, nanoporous and PLL coated nanoporous surface showed about 25 % of differentitation level and had no significant difference between them. The results of the neurite numbers showed very low neurite numbers on smooth surface than that on other surfaces. On the other hand, no obvious effect was found on PLL coated smooth, nanoporous and PLL coated nanoporous surfaces. The results neurite

length also show the shortest neurite length in smooth surface. Interestingly, PLL coated smooth surface had low neurite length compared to nanoporous and PLL coated nanoporous surface. It was found that nanopores enhanced nerite development as long as similar to PLL coated smooth surface while smooth bare surfaces showed very poor differentiation level and neurite outgrowth. These findings suggest that the nanoporous topography did affect neurite development.

The results of this study suggest the effect of the nanoporous SU-8 surface on the in vitro neurite outgrowth of PC12 cells. Therefore, if this nanoporous surface is applied to the surface of implantable neural probe, we could expect the improved results as long-term neuronal recordings than the neural probe with smooth surface. That may because such bioactive surface (nanostructured porous SU-8) is able to allow for neuron to interact with electrode sites (recording sites) which have nano-scale features. By using surface topography, we can to control cell development for biomedical applications not only neural microelectrode and microrobot but also drug delivery and cell guidance, etc.

Keywords: Nanopore, Surface modification, Brain-Machine Interface (BMI), Nanosphere Lithography(NSL)

Contents

List of Figures

1. INTRODUCTION

1.1 Objectives and motivations

Over the past few years, several studies have been made on BMI (Brain-Machine Interface) which

acts as bridge between the central neural system and a physical device like a cochlear implant (CI) or the

Artificial Retina. The BMI technique is required to restore motor and/or sensory functions in patients with

neurological disorders. Microelectrodes for recording brain signals and/or stimulating the brain is required

in the prosthetic devices for restoring human neural, sensory, and motor functions. Thus the microelectrodes

play an important role to transmit the electrical signals between the brain and a prosthetic device. The

function of microelectrodes may be affected by brain tissue reactions to the implanted microelectrodes. For

example, inflammatory reactions affect both the neural tissue and the surface of the microelectrodes, so that

it leads to the formation of glial scar around the implanted microelectrodes. This glia scar acts as insulating

layer and hinder neurons to be recorded or stimulated by microelectrodes. To alleviate this limitation, it is

essential to modify the surface of microelectrodes to enhance the life time. In addition to that, neurite

outgrowth of neurons is expected to have positive effect on the surface of microelectrodes with the suggested

surface modification. The surface modified microelectrodes have great potential for long-term application

for invasive brain machine interface.

The purpose of this work is to fabricate the nano-pore arrays on the SU-8 surface to investigate if the

PC12 cells show affirmative effect on immobilization and differentiation the cells on the nanoporous SU-8

surface. This nanoporous SU-8 surface can be applied to the surface of implantable neural probe. The SU-8 was chosen because it will be used as the substrate and surface of such neural probes in our following works. Compared with silicon based probes, the SU-8 based probes could be more advantageous to alleviate the inevitable small relative motion between the probe and tissues after implantation [1]. The flexibility of SU-8 is less irritating to the cells or tissue than stiff silicon materials. Therefore, a negative photoresist like SU-8 was used for possible flexible microelectrodes instead of silicon wafer. However, the surfaces of currently used neural probes are smooth surface although neurons are known to have positive effect on micro/nano surface structures. Sometimes antibody or nerve-growth factors are coated on the surface of the neural probe to enhance the life-time of the probe. The micro/nano features on the surface of the neural probe could maintain sustainable and long-term effects than the chemical coated surface of that. The physical permanence of micro/nano structures is why the implantable neural probe requires physical surface modification. In this study, we fabricated nano-pore arrays on the surface of flexible SU-8 substrate to find out if we can use the nano-pore array to enhance the neural activities by physical surface modification. We chose the PC12 cells to examine the effect of the nano-pore surface on the *in vitro* neurite outgrowth of neurons. PC12 cells are not neural cells by itself but this cell can differentiate as a neuronal cell by nerve growth factor (NGF) stimulation. For this reason, the PC12 cells have been used as an *in vitro* model to study neural cells [2] such as the test of neural probe and the assessment of neurite outgrowth. Further study would be continued using hippocampal neuron to investigate the effect of the nano-pore arrays on the surface of probe.

1.2 Hypotheses

Neural tissue engineering can be categorized in two-folds: 1) to eliminate defensive encapsulation response

and 2) to promote neuron growth into electrodes. The purpose of this work is to address the second application.

Specific Aim 1: Design a method to fabricate the nano-pore arrays on SU-8 surfaces.

Specific Aim 2: Quantify the effect of nano-porous SU-8 surfaces on the neurite outgrowth of PC12 cells *in vitro*.
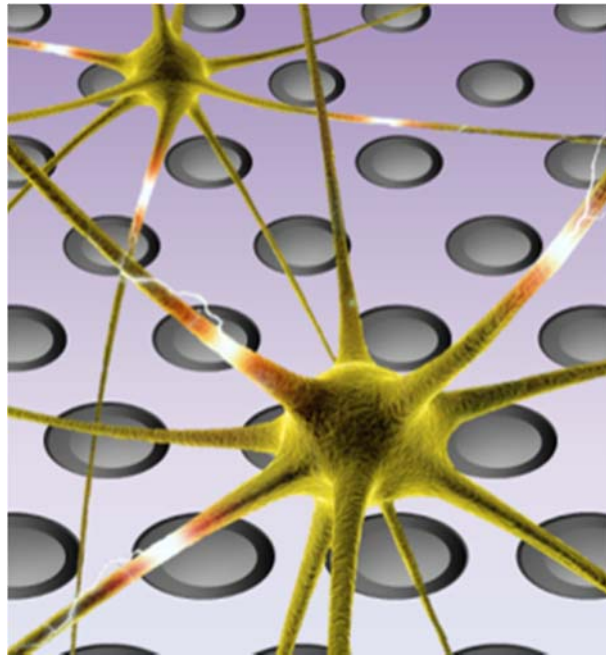
Figure 1.1   Schematic of neurons on the nanoporous surface and interaction between them.

1.3 Background information

1.3.1 Neural microelectrodes

The functions of microelectrode are recording and/or stimulating a specific bundle of neurons by forming a steady interface between neurological and electrical signals. The inception of neural microelectrodes is the metal microwires [3]. This microelectrode has a very simple shape that is one electrode site at the tip of the probe. As the next generation of the microelectrode, several studies have been made on the silicon neural probes according to the development of MEMS (Microelectromechanical Systems) technology. The microelectrode also has been more advanced to enhance the function of microelectrode that record from and/or stimulate the neurons having dimensions that are similar to the magnitude of neurons. The approaches produced multiple insulated metal microwires [4] and micromachined penetrating microelectrode arrays [5, 6] with various substrate materials, insulating dielectrics, and substrate shaping technologies that can be flexible and based on polymers. Furthermore, the Utah array [7], the Michigan array [8] and the new NeuroProbes arrays [9] have been made as the great efforts to reach neurons at the desired three-dimensional position.

In the early times, the use of polymer to the neural microelectrode appears as the insulating layer. For example, polyimide was used to encapsulate the Utah electrodes arrays [10], and parylene C was used to coat the silicon microelectrode [11]. In the recent study, reducing tissue damage caused by the silicon and metals is proposed to be replaced by the flexible polymers as shown in Figure 1.2 [12]. The reason for reducing tissue damage is that they can change their form when the organs deform and the electrodes located on flexible microprobes may evade the gradual movement in the recording site. However, in case of too flexible probes it is difficult to insert them into neural tissues without any other supporting materials or the modification of their ends.

For example, in general, these excessively flexible microelectrodes are made of parylene or polyimide, and need

a more rigid material as support, require the heating of the probe during insertion, or are suitable only for soft

tissues. The rigidity of microelectrodes is determined by the thickness and the elastic modulus of the material.

Polymers such as polyimide and SU-8 are photopatternable and spin coatable, which provides a higher thickness

range compared to parylene, which is evaporated and not photopatternable. However, the baking temperature of

polyimide is much higher than that of SU-8 and this can be a drawback of polyimide. Furthermore, the value for

the elastic modulus for the three of these polymers is between 2 and 5 GPa. This value of silicon and metals is

larger than that of three polymers by two orders of magnitude. For this reason, the polymer based microelectrodes

are being studied.
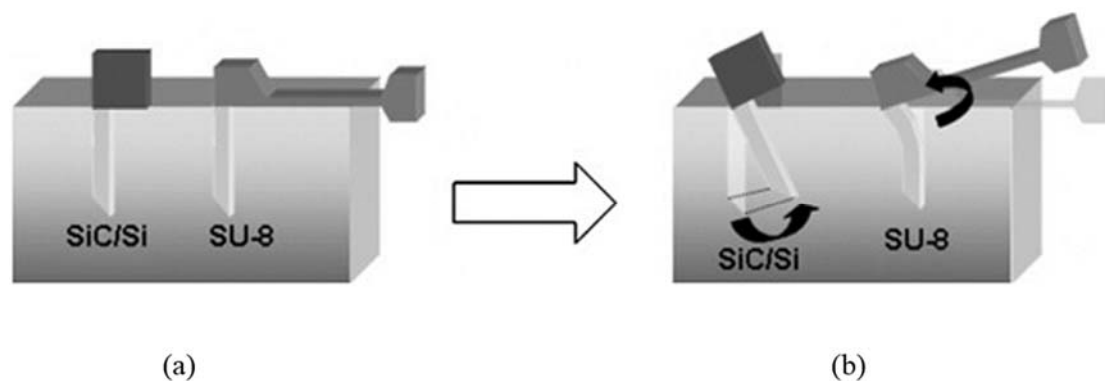
Figure 1.2   (a) Representation of the SiC/Si rigid and the SU-8 flexible microprobes inserted in a tissue. (b) Response of the microneedles when are laterally pushed [12].

1.3.2 The cellular response to implanted microelectrodes

When the microelectrodes is penetrated into the brain, that is a traumatic procedure, some neurons and

glial cells are damaged or killed during insertion, blood vessels are disrupted, and the blood brain barrier is injured

as shown in Figure 1.3a We should be aware that this acute response acts as an important role in two important physiological processes: protection against infectious agents and repair of the damaged tissue. Thus the initial activation and migration of microglial cells are likely beneficial and include production of neurotrophic substances and cell adhesion molecules (CAMs). CAMs support injured neurons and appear necessary for restorative events to take place [13]. However, this largely beneficial initial state usually results in a more adverse long-term response that depends on the extension of the injury. Therefore these reactions often result in damage of neurons and microelectrodes and lead to the proliferation of a glial scar around the implanted microelectrodes as shown in Figure 1.3b. This glial scar prevents neurons to be recorded or stimulated [14]. In this way the outer surface of the neural microelectrodes is frequently surrounded by a dense sheath, which contains markers of macrophages, astrocytes and fibroblasts [15]. This long-term response (Chronic response) results in an increase in tissue impedance, difficulty in the regrowth of neuronal processes and the diminution in the ability to record and stimulate in long-term applications. Controlling the short term response and making the surface more biocompatible for long term will inhibit the glial activation and restrain a glial scar formation.
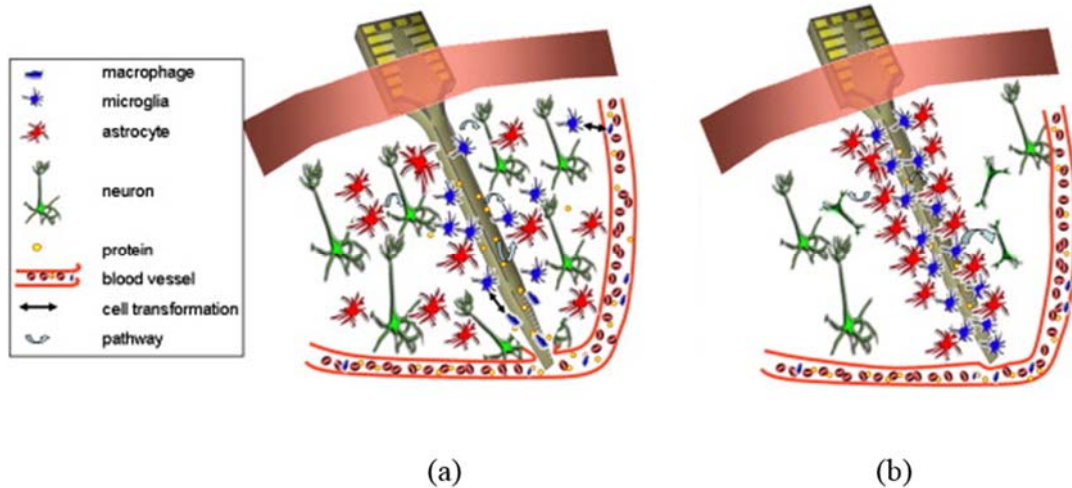
Figure 1.3 Cartoons showing the acute and chronic tissue responses following device insertion. The acute response (a) is characterized by vasculature damage, neuronal injury, plasma protein adsorption, recruitment of activated microglia, and a broad region of reactive astrocyte around inserted devices. The chronic response (b) is characterized by a condensed sheath of cells primarily composed of activated microglia and reactive astrocytes around insertion sites. Degeneration of neuronal processes and additional neuronal loss may also be seen [16].

1.3.3 Re-engineering the cellular response

In the implantable microelectrode study, the method for minimizing the adverse tissue response include the quality of the surgical procedure, the physical dimensions and geometry of the microelectrode, the modification of the surface of microelectrode etc. In this section, we focused on the cellular response on the surface of microelectrode. The aim for the cellular response on the surface of microelectrode to assure that the surface of the microelectrode sustain neurons but does not sustain glial cells. There has been several research on coating the surfaces with bioactive molecules and modifying the surface with polymers or the structure of the surface to regulate the cellular response.

There are generally three approaches to using bioactive molecules to improve microelectrode recording: delivering drugs via microfluidics, systemic injection of drugs to minimize the immunological response, and

attaching biomolecules to the surface through some type of chemical bond (conjugation). Some researchers have attempted to incorporate microfluidics to deliver novel drugs to the insertion position in order to attenuate the biological response to microelectrode insertion [17]. However, since no long term studies of these microfluidics have been completed, there is no way to know if the same cellular processes that physically isolate the microelectrode from the normal cellular environment will occlude these channels and render them useless.

Steroids also have the potential to improve neuronal recordings in vivo because of their ability to reduce inflammation. The effects of dexamethasone, an anti- inflammatory synthetic glucocorticoid was investigated on astrocytes [18]. These studies suggest that dexamethasone has the potential to regulate astrocyte proliferation but additional side effects of this treatment should be studied.

Other group has proposed to immobilize biomolecules on their microelectrodes to mediate the cellular response. Azemi et al., (2008) immobilized L1 molecules—which are neuronal adhesions molecules indicated in the neuronal pathways of mobility and growth—on laminin constructs placed around the microelectrode. The group was successful in promoting the pathways involved with the L1 molecule surrounding the inserted microelectrode. Therefore, they showed better biocompatibility of this surface compared to control groups. However, there is no work in literature of applying this compound to implanted microelectrodes.

The effects of modifying the surface of the microelectrode with surface polymers have also been studied [19]. Electrochemical polymerization was used to deposit both polymer and bioactive molecules onto the surface of microelectrodes to improve the signal conduction at the recording site surface and to attract. These devices were tested both in vitro and acutely in vivo. Therefore, conducting polymers may provide improved interfaces

between microelectrodes and neural tissue but more work is required to better understand this interface and how conducting polymers can improve neuronal recordings chronically.

In vitro studies showed that changes in surface structure on the nano scale level can have an important effect on neurons and glia. The effect of carbon nanofiber coatings was studied on astrocyte proliferation in-vitro [20]. These coatings were either 60 or 200 nm and with either high or low surface energy. These results showed that microelectrode tips coated with fibers of smaller diameter and higher surface energy lead to a decrease in astrocytic adhesion. These cells are one of the primary cells believed to be involved in the encapsulation and isolation of the microelectrode in vivo. Thus, the group concluded that it may be possible to decrease the glial encapsulation of the microelectrode by manipulating the surface structure of the microelectrodes at the nano-scale.

The effect of surface structure was also studied comparing mesostructured porous silicon (PS) to nanostructured porous silicon (PS) as novel surface coatings for ceramic-based microelectrodes [21]. In vitro studies showed that neurons preferred the nanostructured surface by extending significantly more neurites while glial cells avoided the nanostructured surfaces, suggesting that this surface may be useful for targeting appropriate cell types in vivo. Subsequent in vivo studies showed that microelectrodes coated with nanostructured porous silicon could be used to record single neurons. More studies over longer time periods are necessary to determine if these surfaces have a useful effect for improving long-term biocompatibility.

1.3.4 Nanosphere lithography for nanopore arrays

There are several methods to create nanoporous surface. First, to coat porous polymer films on the substrate. This porous polymer films made by using condensing water droplets. After that very well ordered nanoporous

film was fabricated. However, there can be adhesion problem between porous polymer film and the substrate.

Second method is to utilize di-block copolymer lithography. The shape of holes and dots (pillar) made on the substrate by using this technique. However, the size of di-block copolymer is too small less than 30 nm that is smaller than the size of nanopores we want to fabricate. Therefore, nanosphere lithography technique was choose to make the nanoporous topography on the SU-8 film. In 1995, Hulteen and van Duyne pioneered the nanosphere lithography (NSL) [22, 23] to fabricate large area nanostructures by employing commercially available monodisperse polystyrene nanosphers, from 10 nm to several micometers in diameter. The function of NSL relies on a monolayer of monodisperse nanosphers (NSs) on a substrate as a template for thin film deposition or pattern etching. For depositing a nanosphere solution onto the desired substrate, nanospheres is first need to freely diffuse across the substrate, seeking their lowest energy configuration. This is often achieved by chemically modifying the nanosphere surface with a negatively charged functional group such as carboxylate or sulfate that is electrostatically repelled by the negatively charged surface of a substrate such as mica or glass. Nonetheless, the biggest hurdle resides on the preparation of large area monolayer of close-packed NSs on a substrate, which turns out to be a challenging colloidal self-assembly problem.

There are several methods that have been developed to tackle the problem. One is to utilize the depletion force by adding a second species of NSs with smaller size to induce an entropically driven self-assembly of bigger NSs. Nevertheless, a substantial amount of smaller NSs are needed in order to observe the effect. Another method uses the surface tension to assemble the NSs, such as spin coating and vertical pulling. However, they are extremely sensitive to the interfacial properties which are substrate dependent. The resulting NSs packing domains

are usually on the order of a few square micrometers and are susceptible to large cracks and vacancies because of

the instability during the solvent evaporation.

On the other hand, the well-known Langmuir−Blodgett (LB) method [24] assembles the NSs having an

intermediate step in water−air interface, via increasing the NS area fraction either by adding more NSs or by

reducing the confining area. It has also been found that the addition of surfactant can effectively drive the NSs to

assemble into close-packed structure. The disadvantages in the LB method, however, are the strong repulsive

force between NSs coming from the induced charges and the lack of strong binding between NSs. Even with

surfactant, the NS packing structure is hard to maintain while transferring to a substrate that is not sufficiently flat.

In addition, the surfactant greatly reduces the surface tension at water−air interface. Special care on adding

surfactant is needed to avoid the submersion of monolayer NSs.

A new type of self-assembly of NSs has investigated to prepare a monolayer of close-packed NSs that can

be transferred to a substrate of any kind with area size larger than 1 cm^2. This strategy utilizes a modified LB

method with the addition of trace amount of polyethylene oxide (PEO, a long chain polymer with formula

$(OCH_2CH_2)_n$ and molecular weight M_w=145 000 0 g mol^{-1}) in the water. The adsorption of PEO [25] onto the PS

NSs results in the polymer bridging effect which makes the NSs at the water surface to connect through PEO and

form robust NSs membrane against the surface tension tearing during the NSs transfer process.

Moreover, several challenges that are caused in the process of depositing nanospheres via the liquid surface

suspension technique like the LB method could be improved. These problems include the formation of concentric

bi-layer rings and a large number of nanosphere triplets on a second layer on top of the monolayer and domain

dislocations. The strategy to address these issues is to give the substrate an angle of 10° instead of the substrate

being in parallel to the water level. By having the substrate at an angle, the drying plan becomes almost linear and progresses from one end of the substrate to the other as the water evaporates. This means that the nanosphere monolayer forms on the substrate almost row by row rather than forming at different parts of the lattice at the same time. Therefore, this method provides a robust and consistent procedure for creating large scale and high quality polystyrene nanosphere monolayer on the substrate.

Following self-assembly of the nanosphere mask, a metal or other material is then deposited by thermal evaporation, electron beam deposition (EBD), or pulsed laser deposition (PLD) from a source normal to the substrate through the nanosphere mask to a controlled mass thickness. After metal deposition, the nanosphere mask is removed by sonicating the entire sample in a solvent, leaving behind the material deposited through the nanosphere mask to the substrate.

2. MATERIALS AND METHODS

Relevant chemicals and cells are introduced, including the substrates, solvents, and nanoparticles used in this work. Also, experimental techniques relevant to the fabrication, characterization, property analysis of the xxx are explained. In this chapter, the experiment was conducted to verify that PC12 cells are adherent and have extended a large number of neurites on nanoporous SU-8 surface.

2.1 Fabrication of nanopore arrays on SU-8 surface

2.1.1 Materials

Borofloat 33 wafer was obtained from Schott. SU-8 2075 and SU-8 developer was obtained from Microchem Corporation. MA8-GEN3 Mask aligner from Suss Microtec. 5% w/v carboxylate-functionalized polystyrene (PS) nanospheres in deionized water with 0.02% sodium azide were obtained from Spherotech Inc. The mean size of the nanosphere diameter was about 330nm from the manufacturer. Carboxyl group parking area varied from xx $Å^2$/COOH. Polyethylene oxide (PEO) powder with an average molecular weight, MV, of 100,000 was obtained from Sigma Aldrich. Surfactant sodium dodecyl sulfate. Cr etchant (CR-7, Cyantek) was used to remove the chrome layer as a mask.

2.1.2 Fabrication process
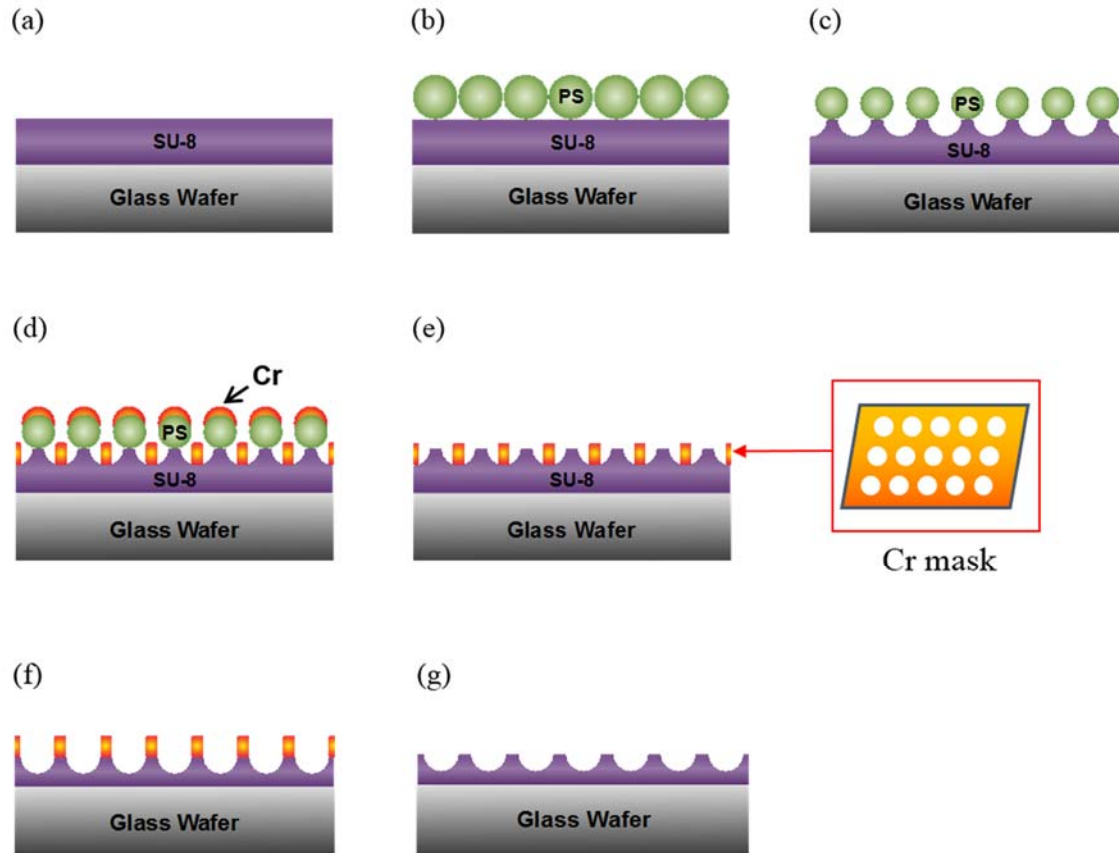
Figure 2.1 Schematic of procedure for fabricating the nanopore arrays on the surface of SU-8: (a) Spin coating of SU-8 on the clean glass wafer; (b) Formation of PS nanosphere monolayer and transfer to SU-8 coated substrate; (c) RIE of PS nanospheres to set final pore diameter; (d) 30 nm Cr evaporation (e) Liftoff by dissolving PS in toluene at 40 °C; (f) RIE of SU-8 through Cr mask (g) Removal of Cr using Cr etchant.

The procedure for fabrication of SU-8 with aligned nanopore array surface is outlined in Figure 2.1, consisting of 7 steps summarized as follows: (a) coating of SU-8 on glass wafer substrates; (b) coating of the monolayer of PS nanospheres onto an SU-8 coated substrate; (c) RIE with O_2 to reduce the diameter of the nanospheres; (d) evaporation of 30 nm Cr; (e) dissolution of the PS nanospheres by sonication in toluene at 40 °C,

leaving a Cr mask over the SU-8 film; (f) O_2 RIE of the SU-8, leaving the desired depth of the holes; (g) removal of Cr mask using CR-7 etchant.

The fabrication process outlined above will now be discussed in more detail. The glass wafer was used as substrates, and SU-8 was used as the surface that the nanopore array are fabricated on its surface. The glass wafer was given an acetone dip (3 min), an isopropanol dip (3 min), and deionized water rinse before application of SU-8 for refreshing surface of the glass wafer. Then, it was heated at 200 °C for at least 45 minutes to a hot plate to remove water from its surface. Afterwards, SU-8 was coated for 45 sec at 4500rpm on the glass wafer, resulting in a film thickness of about 36μm. This procedure was followed by a prebake for three minutes at 65 °C and another nine minutes at 95 °C on a hotplate to evaporate solvent contained in the SU-8. The wafer was exposed with doses about 300 mJ/cm² measured at wavelength of 365nm. Post expose bake was done at 65 °C for 1 min and at 95 °C for 7 min. Development was performed by immersion in SU-8 developer for approximately 4 minutes.

(a)   (b)
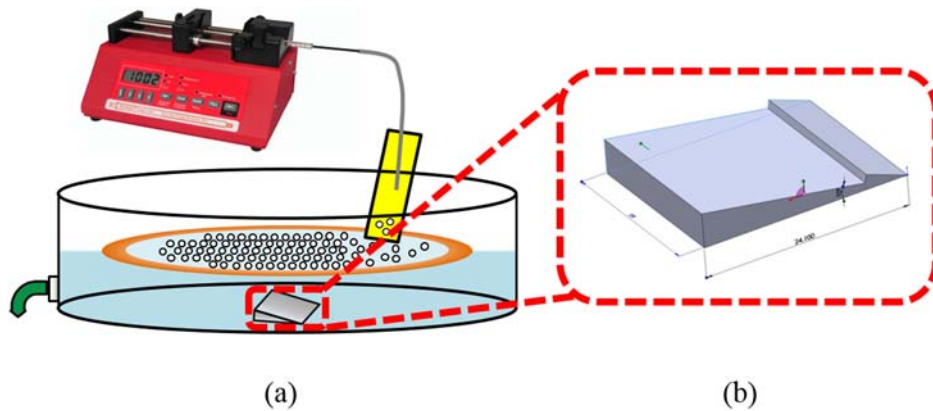
Figure 2.2 Schematic of strategy for the formation of close-paced polystyrene nanoparticles monolayer and the transportation to the substrate at air-water interface. (a) shows experimental set-up for depositing the PS NSs on the substrate using (b) the 10° inclined sample holder laying bottom of petri dish in the water.

After coating SU-8 on the glass wafer, the wafer was cut with about 20 mm x 20 mm pieces. This procedure was followed by the assembly of the PS nanospheres on the surface of the deionized water bath. This step is crucial in creating a well-ordered array. The colloidal PS in water was mixed with ethanol and trace amounts of polyethylene oxide (PEO) powder, creating a solution with lower density than water that spreads across its surface. The PEO serves to bind the particles together as they assemble, creating a more robust monolayer during the subsequent transfer. 5% w/v PS solutions were used with 1:1 ethanol to solution for 200 nm particles. This mixture was then sonicated for 1 minute and continuously dispensed onto a glass slide which had been soaked in a solution containing a small quantity of the surfactant sodium dodecyl sulfate. This procedure ensures a low contact angle, allowing a smooth transition of the particles from the glass slide to the water bath. This is crucial, as the monolayer formation begins as soon as the particles are dropped onto the glass slide and continues as they transfer to the water bath.

After the monolayer was formed, it was transferred to a submerged substrate, a piece (~2 cm^2 in area) of glass, by draining the water bath. The rate at which the monolayer was transferred was controlled by placing the substrate on an RP block with a 10° angle and a small notch to hold the substrate in place while the bath was drained. The experimental setup is shown in Figure 2.2. The draining speed was controlled by a low flow nozzle so that the contact angle progressed across the substrate at a rate of approximately 4 mm/min. With this technique, transfer to hydrophobic substrates such as untreated Si and SU-8 is possible. For faster transfer, the glass piece with SU-8 film was done with an O$_2$ plasma treatment.

The PS diameter was reduced with a reactive ion etching (RIE) step using gas flow rate of 30 SCCM O$_2$, and a chamber pressure at 61mTorr, and a RF power of 50 W for 1 minute. Since the underlying SU-8 layer can

be also etched in this process, for reducing only the PS diameter, selectively, the optimized parameters are required. In general, the diameter of the PS nanospheres can be reduced by up to 50% while maintaining their shape and remaining stable on the underlying pillars.

After reducing the diameter of the PS, a 30nm thick layer of chromium was deposited on the sample as an etching mask layer using an electron-beam evaporation system with the ratio of 2 Å sec^{-1}. Following this, the sample was soaked ultrasonically in toluene at 40 °C for 1 h [26] to remove the PS nanospheres from the SU-8 layer and was cleaned with dipping into IPA for 3 minutes and deionized water for 3 minutes. After that, the hole-shaped Cr patterns were obtained and used as a hard etching mask while etching SU-8. The protruding SU-8 region, not covered by the Cr mask layer, was etched by RIE using gas flow rate of 40 SCCM O_2, a chamber pressure at 61mTorr, and a RF power of 40 W for 4 minutes.

Finally, the Cr mask was removed with a Cr etchant (etch rate: 800 Å min^{-1}), leaving the corresponding hole patterns on the surface of SU-8. In fact, in the experiment, after one minute the chrome was removed from the sample. Since the sample is transparent, the process of removing the chrome was visibly observed. The final diameter of SU-8 hole is determined primarily by the final diameter of the PS particles achieved in the first RIE step.

2.1.3 Evaluation of surface structure by SEM or AFM

Scanning electron microscope (SEM) is very useful tool for analyzing the structure of surface. SEM has some requirements on sample type and sample preparation. The sample has to be clean and dry, it can't be volatile or include dissolved gas which could be released. The conductivity of the sample is also important because a

nonconductive material causes charging which weakens the quality of the image. That is why the samples must be coated with a thin layer of carbon, gold or gold-palladium mixture [27]. In this study, we used platinum sputter to generate a conductive thin layer on the samples. Fabricated nanoporous SU-8 samples were imaged by a Hitachi S-5200 field emission scanning electron microscope. Sample imaging was made with mainly 3 kV acceleration voltage, spot size and used magnification varied depending on being observed surface conditions.

The atomic force microscopy (AFM) is the most widely used instrument among recently introduced scanning probe microscopy (SPM) techniques. The widespread use of the AFM is attributed to the accurate three-dimensional reconstruction of the sample topography with atomic resolution for a relatively low cost and within a short time. Another important reason for using this characterization is that there is almost no restriction on the sample to be analyzed. Furthermore, the AFM data contain important information for structural analysis of the surface. In this study, the images of poly-L-lysine coated smooth and uncoated nanoporous SU-8 surfaces were employed in non-contact mode (NCM) to measure the surface roughness using AFM (NX10, Park System Corp., Korea). All measurements were performed in air at room temperature. The typical scan size was of $5 \times 5\ \mu m^2$.

2.2 PC12 cell culture test

2.2.1 Materials

PC12 cells (CRL-1721 ATCC, Manassas, VA, USA), rat pheochromocytoma cells derived from adrenal medulla, were grown on poly-L-lysin(0.01%; Sigma Chemical Co., St. Louis, MO, USA) -coated dishes in RPMI-1640 supplemented with 10% horse serum, 5% fetal bovin serum (FBS) (SH30919.03 Hyclone, Thermo Fisher Scientific Pittsburgh, PA, USA), and 1% antibiotics at 37 °C with air containing 5% CO_2. For differentiation study,

PC12 cells were plated on the substrates and treated by NGF (100 ng/ml; BD biosciences, Two Oak Park, Bedford, USA) supplemented medium for 7 days. And this NGF supplemented medium was changed three times during differentiation.

2.2.2 Preparing substrates for cell culture

Before cell culture was conducted, ethanol was used for the sterilization of the sample. Autoclave treatment for the sterilization induced that SU-8 exfoliated from the glass substrate. PC-12 cells were used at passage numbers less than 20.

Substrate Sterilization: All the substrates were sterilized for cell culture using the basic sterilization techniques, ethanol treatment. SU-8 nano- and smooth film coated on glass substrates were sterilized in 99% ethanol for 24 hours in the dark. Stirrer speed was at 50 rpm. After ethanol treatment, in a laminar hood, the substrates were washed with sterile deionized water three times and then dried spontaneously. The reason these substrates were sterilized in ethanol is that heat sterilization (autoclaving) introduced cracks and pitting on these SU-8 coated substrates leading to the peeling off the SU-8 layer.

Chemical Treatment of Substrates: Cell adhesion is dependent on proper anchorage of cells to the growth surfaces. For most cell lines, and especially for post-mitotic neurons, coated cell culture plates are prerequisite for seeding. The most commonly used coating reagents are positively charged polymers such as poly-L-lysine or biologically purified adhesive molecules such as collagen.

One group of smooth SU-8 substrates and the other one group of nanoporous SU-8 substrates were treated with 0.1% poly-L-lysine for 24 hours in a CO_2 incubator (37 °C; 5% CO_2 in air). These substrates were then

washed with sterile deionized water three times. The reason for choosing poly-L-lysine is that this treatment does

not induce focal adhesions [28, 29] but instead it generates ionic bonds to cells. Its working principle is that the

polycationic poly-L-lysine molecules adsorb strongly to various solid surfaces, leaving cationic sites which

interact by means of electrostatic interactions with the anionic sites on the cell surfaces [30, 31]. Sine poly-L-

lysine is a synthetic molecule, it does not bind to chemically specific receptors to stimulate biological activity

other than those elicited by physical interactions with the substrate. In addition, poly-L-lysine does not have the

impurities that are commonly present in natural polymers.

2.2.3 PC12 cell culture

Cell culture – Maintenance: PC12 cells were seeded and cultured in a stock dish and allowed to reach

confluence in an undifferentiated state (without NGF) and were split every 3-4 days. These cells will differentiate

into sympathetic-neuron like form when exposed to nerve growth factor (NGF) [32], thus neurite development in

PC12 cells upon NGF exposure was investigated. NGF was added to elicit neurite growth in all experiments. Cell

cultures were maintained at 37 °C in a humidified atmosphere of 5% CO_2 /95% air for seven days in all

experimental studies. Cells were counted using a hemacytometer before seeding them in all the experimental

groups.

Cell culture on the smooth or nanoporous SU-8 substrates: Cells were seeded in triplicates at a seeding

density of 1.5×10^5 cells/cm^2 on all substrates for optical microscope and SEM analysis of neurite development.

The different types of substrates for both types of analysis were set up in parallel and maintained in the same

culture dish and hence received the same culture conditions. Any differences in culture media, NGF addition and

incubator conditions hence were not a factor that might influence the measured neurite development after 1 week

of culture. The cells were maintained in culture as mentioned in the previous section (Cell Culture - Maintenance).

2.2.4 Image analysis

Neurite samples chosen for the number and length assay measurements were those extending from single

cells and from aggregates present within the field of view. Three randomly chosen visual fields with at least 100

randomly selected cells were scored using an optical microscope. Using ImageJ software, PC12 neurite number

and mean length assays were quantified every other day for a week, with mean lengths determined by an average

end to end measurement of at least 30 random neurites.

2.2.5 Reverse Transcriptase (RT)-Polymerase Chain Reaction (PCR) for NSE

To determine the NSE in PC12 and differentiated PC12, reverse transcription polymerase chain reaction

was used. Total RNAs from PC12 cells and differentiated PC12 cells on bare SU-8, PLL coated SU-8, nanoporous

SU-8 and PLL coated nanoporous SU-8 were prepared using TRIzol reagent (Invitrogen, Carlsbad, Calif). 0.5 μg

of purified total RNA was used for RT. NSE mRNA expression was examined by PCR to amplify the NSE

sequence. For quantification, rat Cyclophilin A mRNA expression was analyzed.

### 2.2.6 Cell culture sample preparation for SEM analysis

For the SEM analysis, after seven days of culture the cells were fixed in 1:1 methanol and acetone mixture

at -20°C for about 30 minutes and at -80°C overnight. SEM images of neurite of neuron cultured on each sample

condition (uncoated smooth bare, poly-L-lysine coated smooth, uncoated nanoporous and poly-L-lysine coated

nanoporous SU-8 surfaces) were acquired with a Hitachi S-4800 field emission scanning electron microscope. All

samples were sputter coated with 10 nm of platinum prior to taking SEM images. The characterization of the

cellular morphology (neurite and the end part of neurite) for PC12 cells on each surface condition was investigated
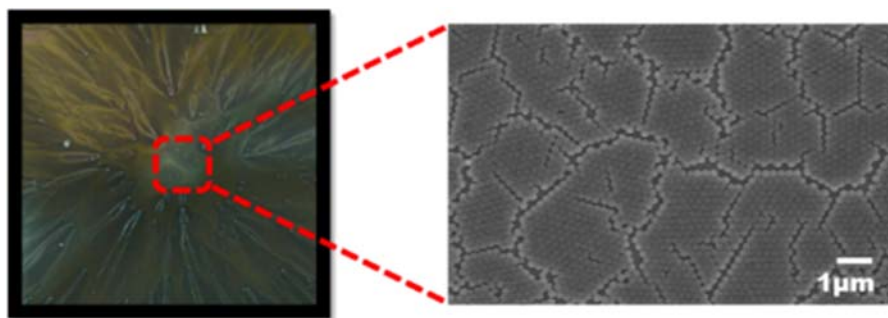
based on the SEM images.

3. CHARACTERIZATIONS OF NANOPORES
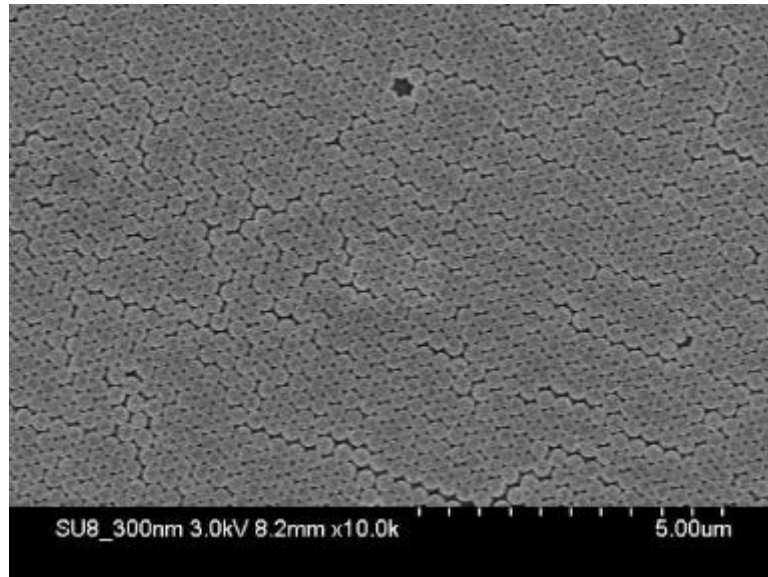
**Figure 3.1**   SEM image of the deposited PS on the SU-8 surface on top of the glass substrate.

Transfer of Monolayer PEO/PS NSs Hybrid on s Substrate. The monolayer NSs can be transferred onto

a SU-8 coated glass substrate by slowly draining the water while still keeping its original packing structure. Figure

3.1 show the SEM images of monolayer of close-packed PEO/NSs hybrid with diameter 300 nm, on SU-8 film

(SU-8 coated glass substrate) prepared as mentioned in Materials and Methods (Fabrication Process). The nearly

defect free area is bigger than 30 μm × 30 μm for 300 nm NSs. The three main defect types that occur in these

arrays can be observed, consisting of missing particles, particles that are too small or too large, and domain

dislocations, or cracks in the array. In the next chapter, these problems were discussed.

To achieve clean and hydrophilic surfaces is a prerequisite for arranging the spheres orderly by providing a small contact angle, which allows the solution to be deposited on the substrate surface uniformly. In case of applying spin coating to the SU-8 surface, it is difficult to deposit the well-ordered PS monolayer array on the surface of SU-8 because the surface of SU-8 is rugged and hydrophobic. It was observed that a lot of domain dislocations, or cracks in the array that deposited by spin coating as shown in Figure 3.2. For the problems mentioned in previous chapter, first, missing particles are related to the initial PS particle concentration; too low a concentration leads the void defects and too high a concentration results in particles scattered on top of the array. However, even with optimal concentration both defects types still occur in some areas. The range of particle size depends on the process used to fabricate them. A coefficient of variation of less than 2% is typical from most suppliers, but this error typically becomes worse for smaller diameter nanospheres. Domain dislocations most likely arise due to small disturbances during the transfer of the monolayer to the substrate. All of these defects are controlled well enough that they are not visible to the naked eye.


Figure 3.2   Photograph and SEM image of the PS array on the surface of SU-8 after spin coating.

In order to form periodic nanoporous structures with a 300 nm diameter, a single-layered polystyrene nanospheres array was coated on the surface of SU-8 and then oxygen RIE was applied to the array to provide a space, which was filled with chrome as a mask.


(a) (b)
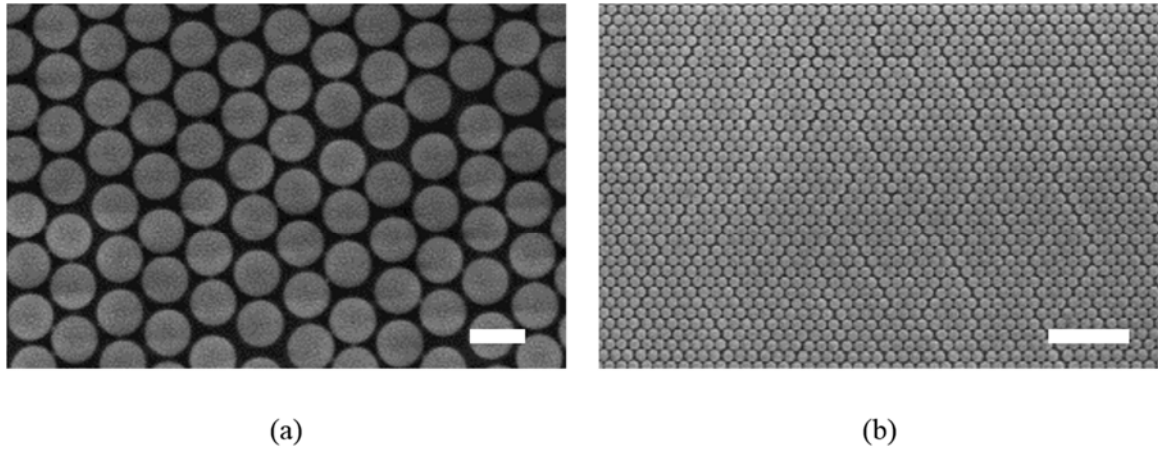
Figure 3.3   SEM images of top view after a 60s O_2 etch starting with 300 nm PS particles. The scale bars represent 300 nm (a) and 2 μm (b), respectively.
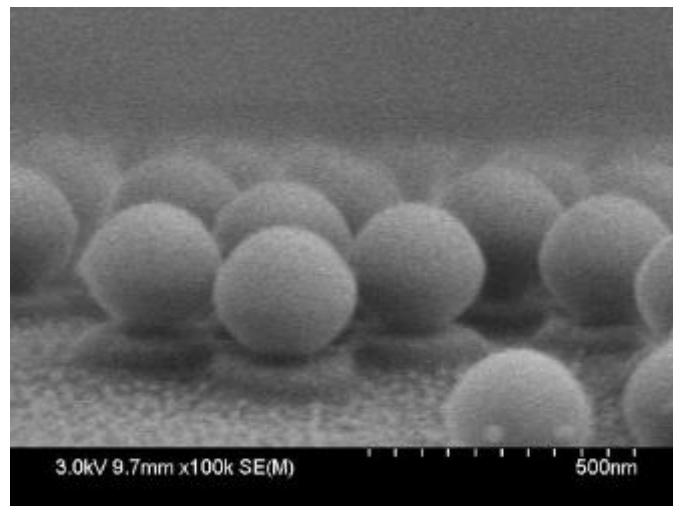
Figure 3.4   SEM image of the SU-8 side view surface after a 60s O_2 etch.

Polystyrene etching. Figure 3.3 shows the shapes of the polystyrene nanospheres and the diameters, which

changed after the oxygen RIE process. Figure 3.4 shows that the SU-8 underlayer was affected by the O_2 plasma.

The PS nanospheres can be etched to roughly 50 % of their original diameter before losing their shape.
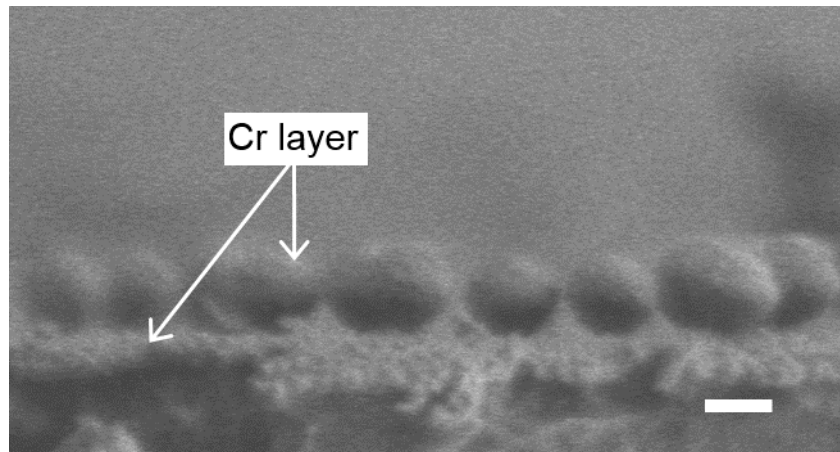

Figure 3.5　A SEM image of side view of SU-8 surface after evaporation of 30 nm Chromium. The scale bar

represents 200 nm.

After the PS diameter reduction, the evaporation of 10 nm Cr step was followed as shown in Figure 3.5.

After the deposition processes, the samples were washed ultrasonically in toluene heated to 40 °C for 1 h to

remove the residual nanospheres. The SU-8 underlayer was then etched using RIE.

When the PS is dissolved in toluene heated to 40 °C, the remaining holes in the Cr layer have a small ridge

due to the etching of the underlying SU-8 layer. This gap is essential for PS particles that have been etched closed

to the 50% limit, as it creates a separation between the PS and SU-8 during the Cr evaporation, allowing the

toluene to reach the PS during the liftoff step.

Final nanoporous structure. After all the processes had been carried out, SU-8 nanoporous structures came into sight. Figure 3.6 shows SEM images that the nanoporous arrays were successfully achieved by means of NSL techniques using polystyrene nanospheres. The pores had dimensions of about 200 nm (Figure 3.6a) in diameter and about 96 nm in separation. The pores are approximately 280 nm deep (Figure 3.6b). Figure 3.6c shows the image with 20 degrees of axial tilt in cross section.

(a)   (b)

(c)
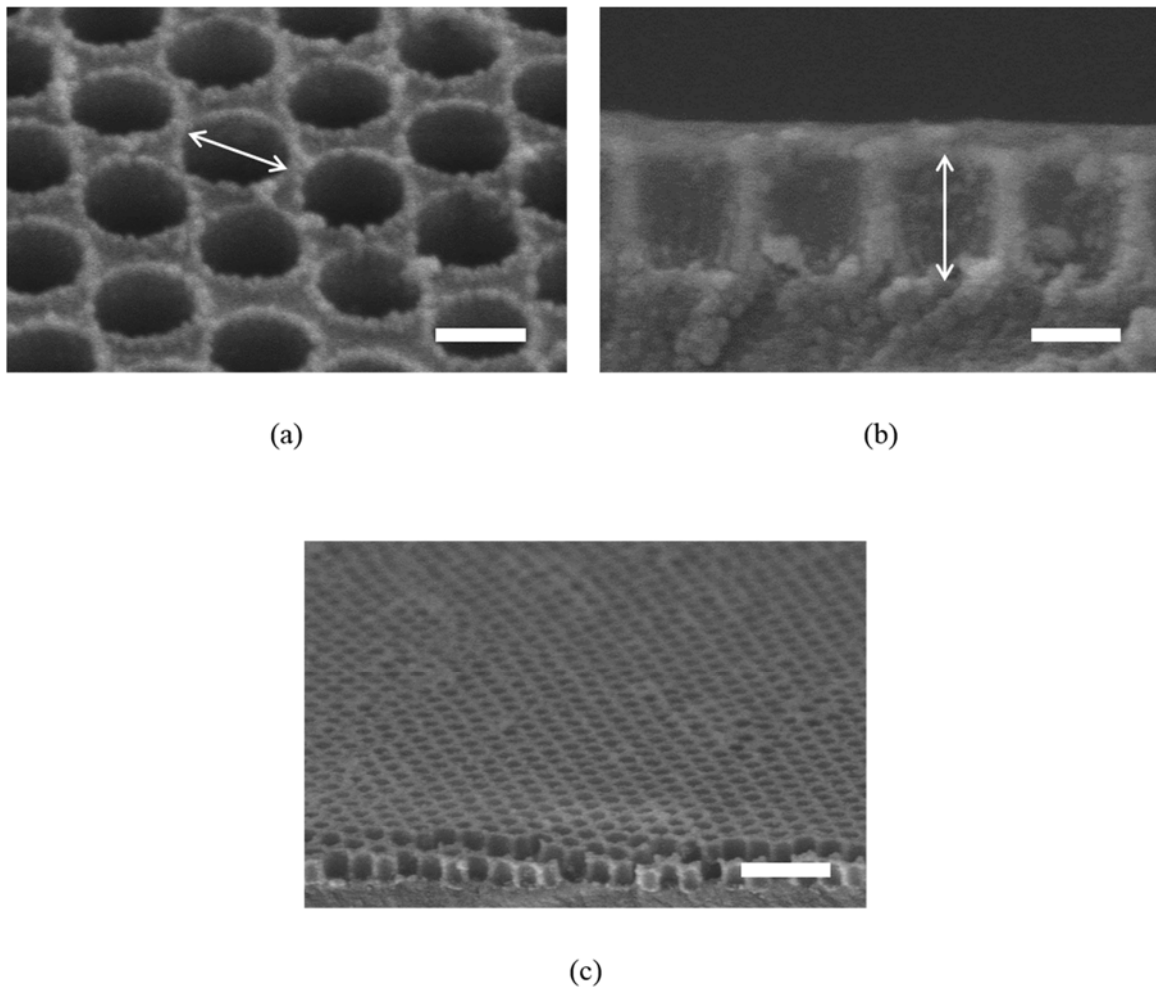
Figure 3.6   SEM images of the nanoporous arrays on the SU-8 surface. The scale bars represent 200 nm (a, b) and 1 μm, respectively.

Figure 3.7 shows the surface topography on prepared PLL coated smooth (a) and uncoated nanoporous (b)

SU-8 surface. In Figure 3.7a, surface roughness (R_q) was about 7.25 nm. Since, R_q are the most widely used a

surface parameter, it was selected to express the surface roughness in this study. In Figure 3.7b, the nanopores had

dimensions of 200 nm in diameter, 296 nm in periodicity. These diameter and periodicity of nanopores obtained

from the AFM image have good agreement with the measured results by SEM as shown in Figure 3.7b.

(a)   (b)
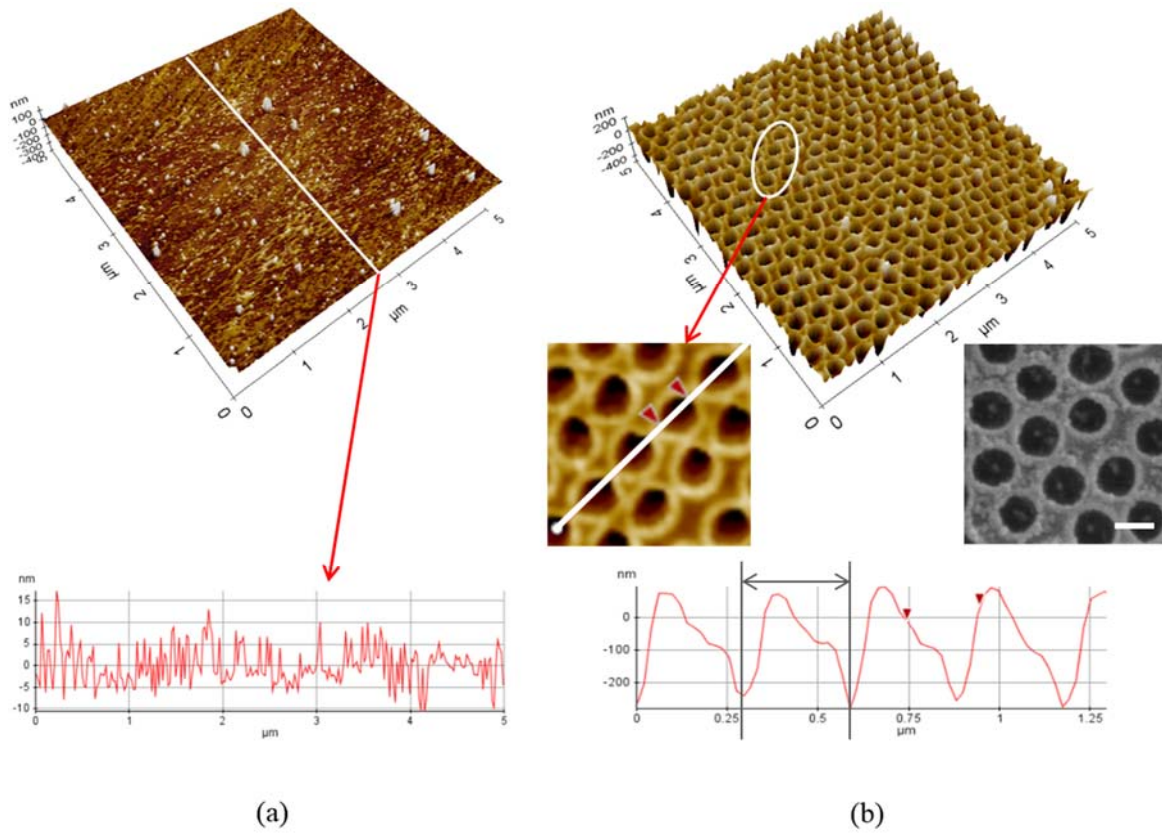
Figure 3.7   Surface topography of the prepared surfaces: (a) poly-L-lysine coated smooth SU-8 surface (AFM image and the surface profile corresponding to the solid line in white); (b) uncoated nanoporous SU-8 surfaces (AFM and FE-SEM images). The surface profile in (b) shows the diameter and the periodicity of the nanoporous surface corresponding to the solid line in white. The scale bar in SEM image represents 200 nm.

4. RESULTS OF PC12 CELL OUTGROWTH

Light microscope observation. Figure 4.1 shows micrographs of PC12 cells cultured for 1 day in the presence of NGF on four types of surfaces. Figure 4.1a shows that PC12 cells were not adherent and remained in a spherical shape on smooth SU-8 surface that was not coated with poly-L-lysine. In contrast, after 1-day culture, some PC12 cells on PLL coated smooth, uncoated nanoporous, and PLL coated nanoporous SU-8 surfaces changed from spherical to flat. The number of neurite-bearing cells on nanoporous (Figure 4.1c) and PLL coated nanoporous (Figure 4.1d) SU-8 surfaces were less than that on PLL coated smooth SU-8 surfaces (Figure 4.1b). Figure 4.2 shows four micrographs of PC12 cells cultured for 3 days on four different types of surfaces. Figure 4.2a shows non-adherent and undifferentiated PC12 cells on smooth bare SU-8 surface. The number of neurite-bearing cells on PLL coated smooth (Figure 4.2b), uncoated nanoporous (Figure 4.2c), and PLL coated nanoporous (Figure 4.2d) SU-8 surfaces were more than that on respective surfaces for 1 day. The neurite lengths of PC12 cells cultured on three types of surfaces except for smooth bare SU-8 surface were slightly longer than that on respective surfaces for 1 day.
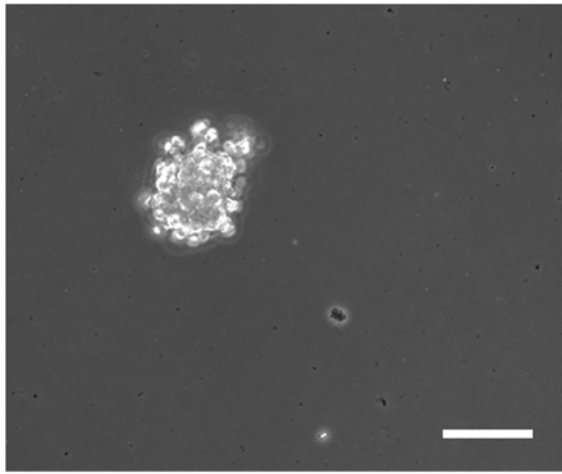
In Figure 4.3, micrographs of PC12 cells cultured for 5 days on four types of surfaces. In case of smooth bare surface, cells were still remained a spherical shape. The number of neurite-bearing cells on PLL coated smooth (Figure 4.3b), uncoated nanoporous (Figure 4.3c), and PLL coated nanoporous (Figure 4.3d) SU-8 surfaces also seemed more than that on respective surfaces for 3 days. The neurite lengths of PC12 cells cultured on uncoated nanoporous (Figure 4.3c) seemed slightly longer than that on PLL coated smooth (Figure 4.3b) and

PLL coated nanoporous (Figure 4.3d) SU-8 surface. In Figure 4.4, micrographs of PC12 cells cultured for 7 days

on four types of surfaces. On smooth bare SU-8 surface, PC12 cells were not differentiated. The trend of cell

differentiation on all surfaces seemed similar in case of 5 days. An exact value for differentiation level was in

quantitative analysis. The neurite lengths of PC12 cells cultured on PLL coated nanopores (Figure 4.4d) seemed

slightly longer than that on PLL (Figure 4.4b) and nanoporous SU-8 surface (Figure 4.4c).
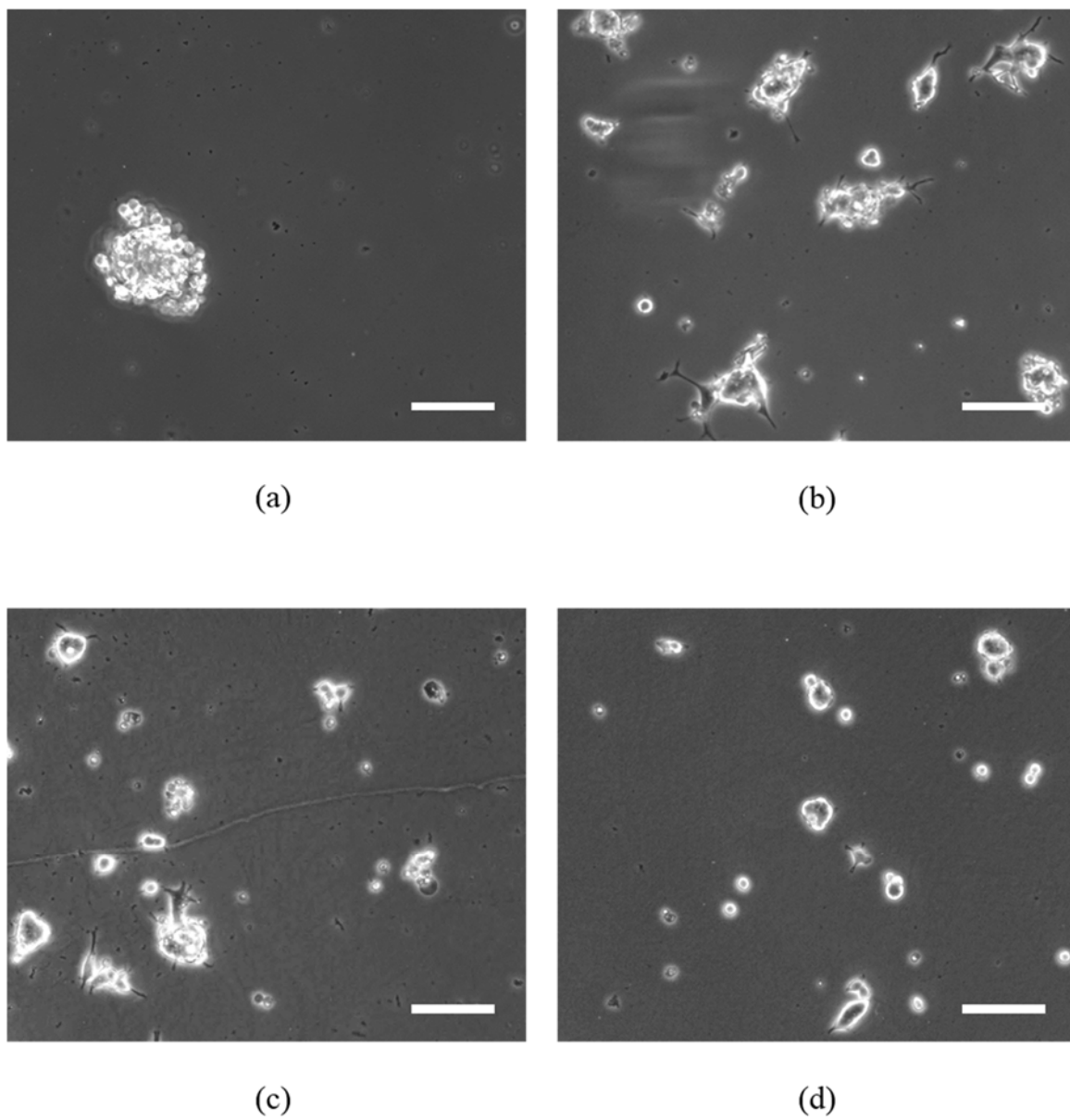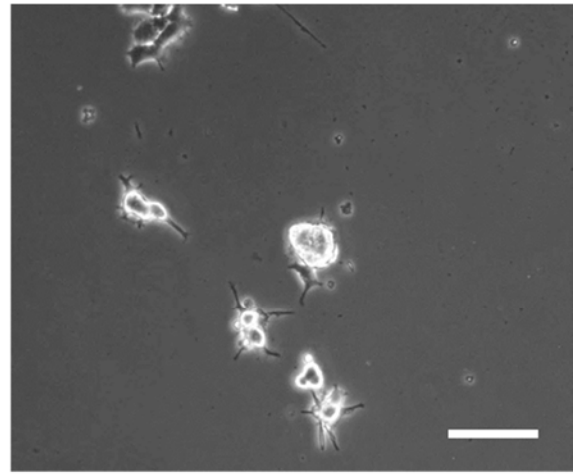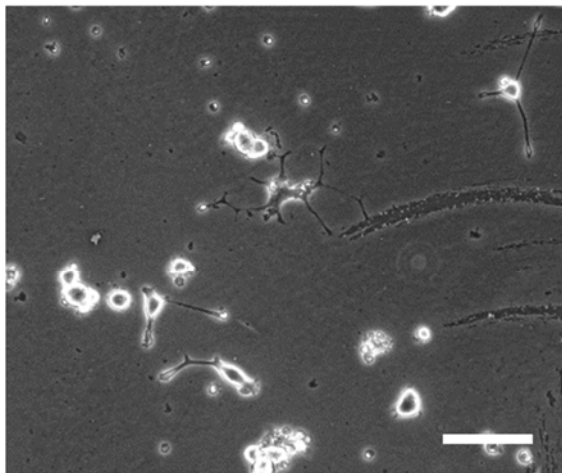
Figure 4.1 Microphotographs of 1-day-cultured PC12 cells on uncoated smooth bare (a), poly-L-lysine coated smooth (b), uncoated nanoporous (c) and poly-L-lysine coated nanoporous SU-8 surfaces. The scale bar represents 100 μm.

Figure 4.2 Microphotographs of 3-day-cultured PC12 cells on uncoated smooth bare (a), poly-L-lysine coated smooth (b), uncoated nanoporous (c) and poly-L-lysine coated nanoporous SU-8 surfaces. The scale bar represents 100 μm.
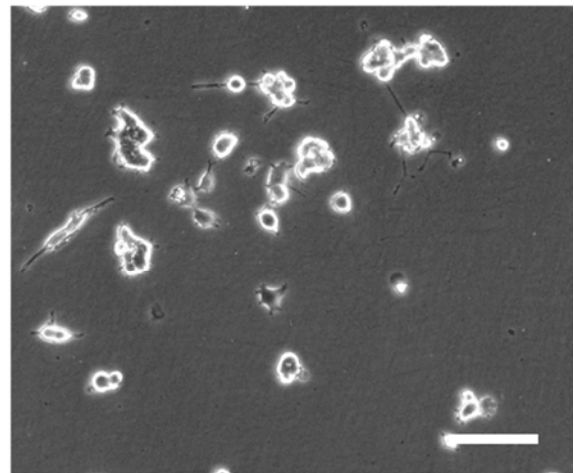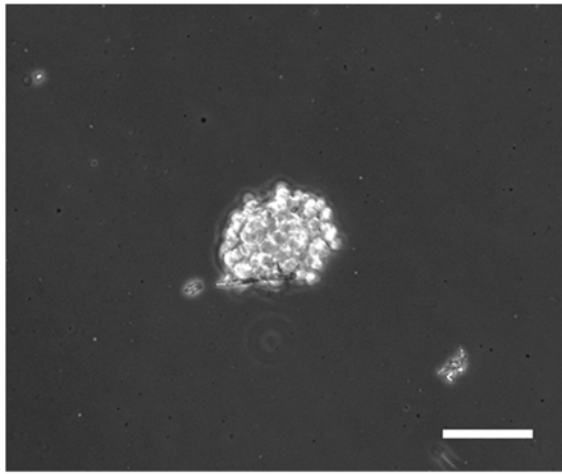
Figure 4.3 Microphotographs of 5-day-cultured PC12 cells on uncoated smooth bare (a), poly-L-lysine coated smooth (b), uncoated nanoporous (c) and poly-L-lysine coated nanoporous SU-8 surfaces. The scale bar represents 100 μm.
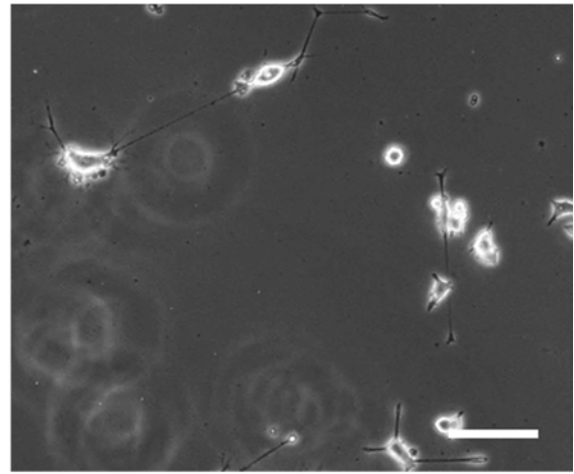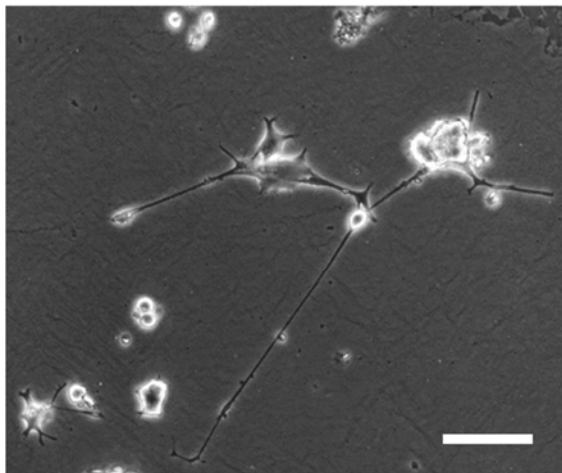
Figure 4.4 Microphotographs of 7-day-cultured PC12 cells on uncoated smooth bare (a), poly-L-lysine coated smooth (b), uncoated nanoporous (c) and poly-L-lysine coated nanoporous SU-8 surfaces. The scale bar represents 100 μm.

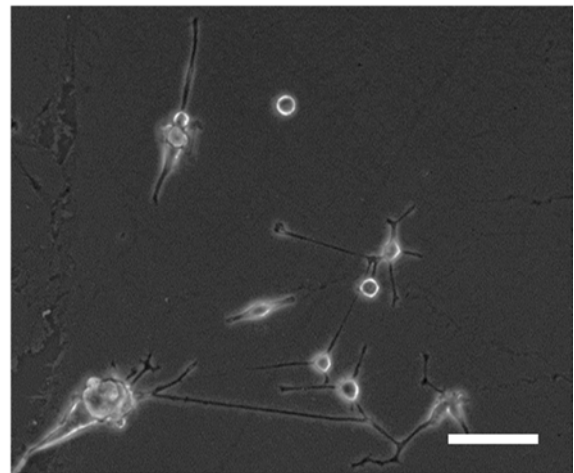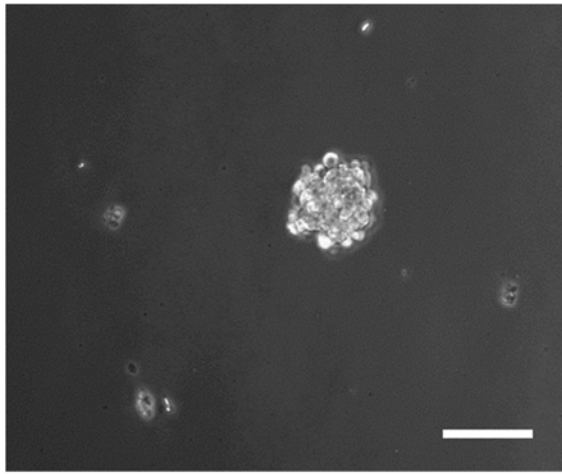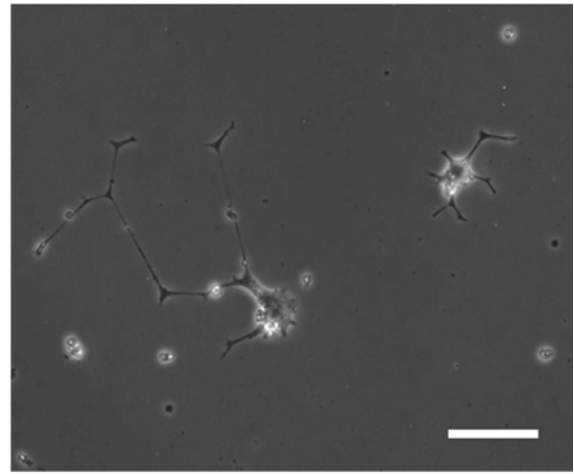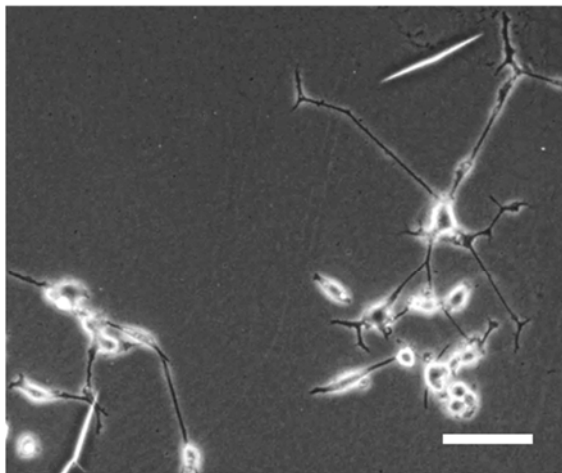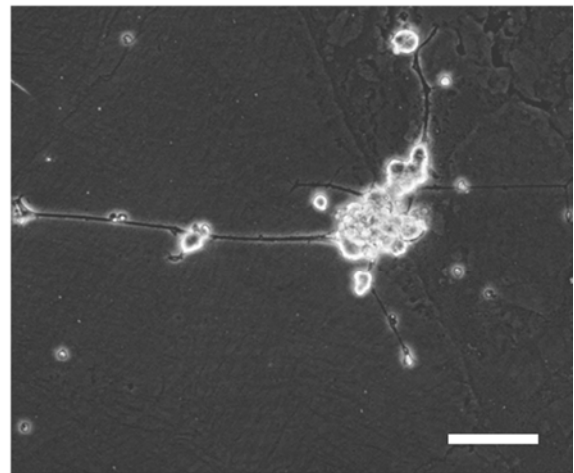**Neuronal Differentiation of PC12 Cells.** To perform a quantitative analysis of neuronal differentiation of PC12 cells, RT-PCR was used to analyze the expression of a neuronal marker (NSE). PCR results was calculated as the rates of NSE mRNA expression out of the Cyclophilin A mRNA expression at each culture day as shown in Figure 4.5. Figure 4.5a shows the lowest differentiation level compared to other surfaces. PCR results after 5 and 7 days' culture show that PC12 cells were slightly differentiated on smooth bare SU-8 surface. The expression level of NSE of PC12 cells on PLL coated smooth (Figure 4.5b) and uncoated nanoprous (Figure 4.5c) SU-8 surface were prone to increase gradually between 1 and 7 days. Cells on PLL coated nanoporous (Figure 4.5d) SU-8 surface after 5 days' culture showed maximal levels of NSE expression. These results suggest that the expression level of NSE of PC12 cells means the degree of neuronal differentiation and would be similar to the results on differentiation level through image analysis in bright-field micrographs of PC12 cells during culture days.

To quantify the differentiation level of PC12 cells in micrographs, first, cells with neurites length longer than 25 μm were defined as differentiated cells. Differentiation levels of PC12 cells were calculated as the percentage of the differentiated cells out of the total cells on the surfaces. Apoptotic and damaged cells were not included in the count. Figure 4.6 shows the differentiation level of cells on different type of surfaces. Figure 4.6a was 0.0%, 0.0%, 1.5±1.3% and 1.1±1.1% for PC12 cells on the smooth bare SU-8 surface after 1, 3, 5 and 7 days' culture, respectively. Figure 4.6b was 4.0±1.7%, 18.0±2.5%, 27.2±6.9% and 25.6±3.5% for PC12 cells on poly-L-lysine coated SU-8 surface after 1, 3, 5 and 7 days' culture, respectively. Figure 4.6c was 2.1±0.5%, 10.9±1.8%, 21.5±4.1% and 26.6±2.7% for PC12 cells on uncoated nanoprous SU-8 surface after 1, 3, 5 and 7 days' culture, respectively. Figure 4.6d was 2.4±0.9%, 10.6±2.3%, 19.5±2.9% and 24.5±4.9% for PC12 cells on PLL coated

nanoprous SU-8 surface after 1, 3, 5 and 7 day's culture, respectively. At all the time points, the differentiation

level of PC12 cells is significantly greater on PLL coated smooth (Figure 4.6b), uncoated nanoporous (Figure

4.6c), and PLL coated nanoporous (Figure 4.6d) SU-8 surfaces relative to smooth bare SU-8 surface. Among three

types of surfaces except for smooth bare SU-8 surface, PLL coated smooth SU-8 surface (Figure 4.6b) had a

higher differentiation level compared to uncoated nanoporous (Figure 4.6c) and PLL coated nanoporous (Figure

4.6d) SU-8 surface. The highest percentage of differentiation achieved in the study, about 27%, was observed for

PC12 cells on PLL coated smooth (Figure 4.6b) SU-8 surface after 5 days' culture. This maximal level of

differentiation did not increase significantly for remainder of the study, that is, after 7 days' culture. On the other

hand, differentiation levels of PC12 cells cultured on uncoated nanoporous (Figure 4.6c) and PLL coated

nanoporous (Figure 4.6d) SU-8 surface increased gradually between 1 and 7 days. These results suggest that

uncoated nanoporous SU-8 surface has similar effect of differentiation compared to poly-L-lysine coated smooth

SU-8 surface. Furthermore PC12 cells on smooth SU-8 surface were hardly ever differentiated.
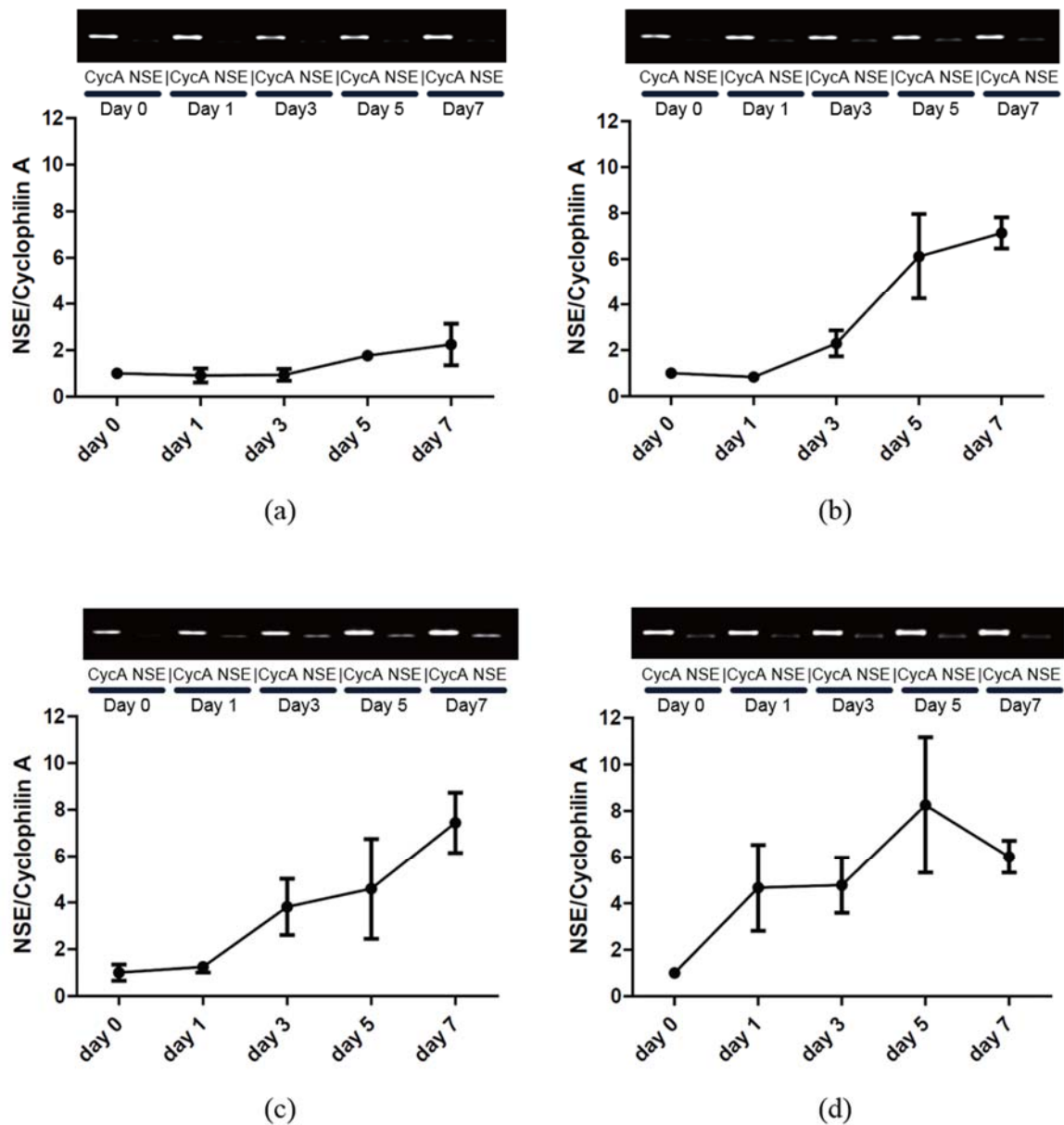
Figure 4.5 Changes in NSE expression were assessed by RT-PCR for 7 days' culture on uncoated smooth bare (a), poly-L-lysine coated smooth (b), uncoated nanoporous (c) and poly-L-lysine coated nanoporous (d) SU-8 surfaces. PCR results was calculated as the rates of NSE mRNA expression out of the Cyclophilin A mRNA expression at each culture day.
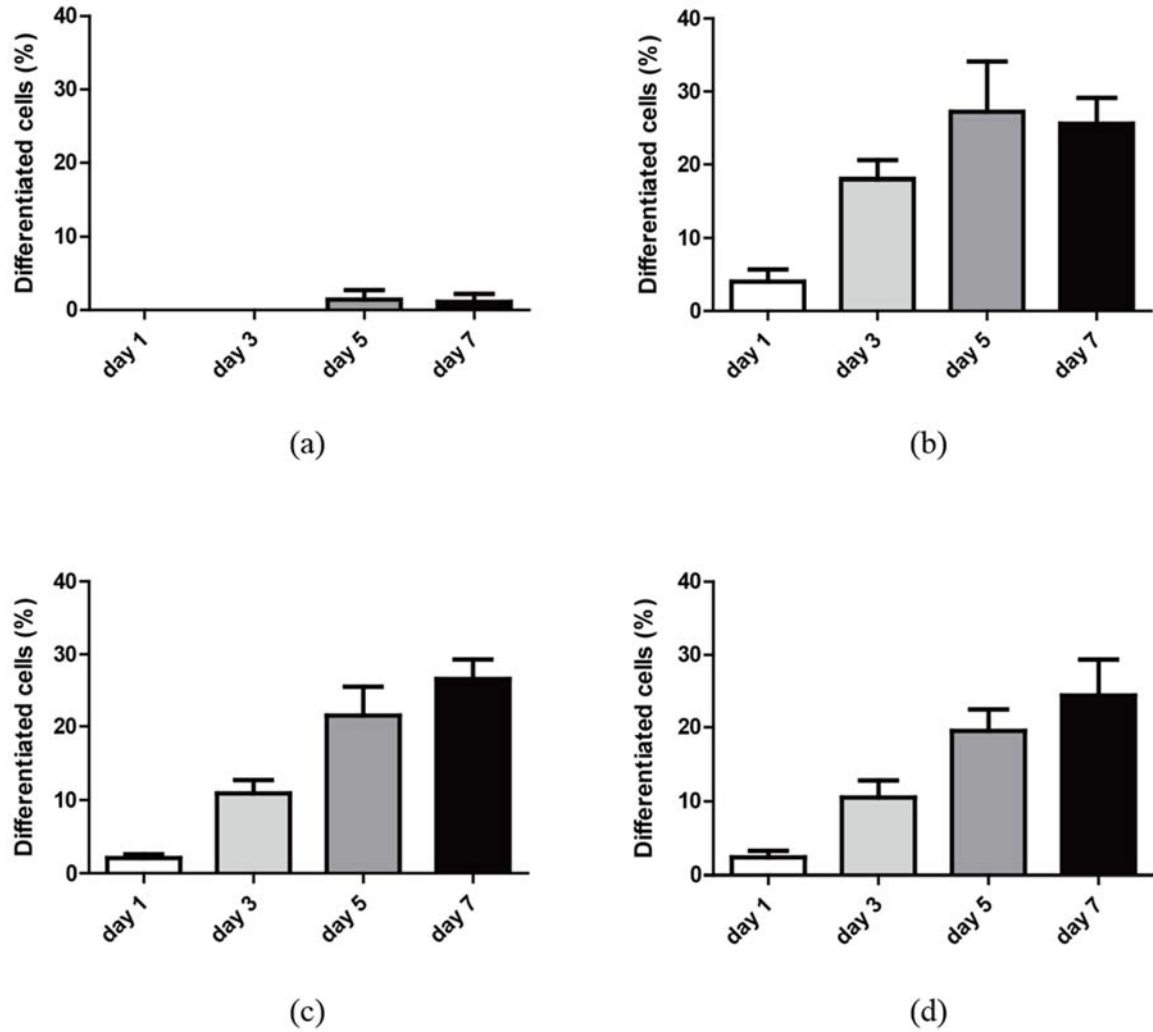
Figure 4.6 Bar graphs show the quantitative analysis of the differentiation level of PC12 cells on surfaces with different topography. Cells cultured on: (a) uncoated smooth bare; (b) poly-L-lysine coated smooth; (c) uncoated nanoporous; (d) poly-L-lysine coated nanoporous SU-8 surfaces. Differentiation levels of PC12 cells were calculated as the percentage of the differentiated cells out of the total cells on the surfaces. Values reported are mean ± standard error.

Quantification of Neurite Development. To quantitative analysis of neurite development the number of neurites was counted and their lengths were measured from three replicates for each type of surface from both types of analyses. With all the measurements pooled together from the triplicate cultures for each type of surface, the means and standard errors of the neurite length and the neurite numbers for each type of surface were calculated. Figure 4.7 shows the neurite numbers per a PC12 cell on the four types of surface. Figure 4.7a shows that the mean neurite numbers was 0.0, 0.0, 0.2±0.1 and 0.2±0.2 (neurites/cell) for PC12 cells on the smooth bare SU-8 surface after 1, 3, 5 and 7 days' culture, respectively. Figure 4.7b was 1.0±0.3, 1.4±0.1, 1.6±0.2 and 1.5±0.2 (neurites/cell) for PC12 cells on poly-L-lysine coated SU-8 surface after 1, 3, 5 and 7 days' culture, respectively. Figure 4.7c was 0.8±0.2, 1.3±0.1, 1.3±0.1 and 1.5±0.1 (neurites/cell) for PC12 cells on uncoated nanoprous SU-8 surface after 1, 3, 5 and 7 days' culture, respectively. Figure 4.7d was 0.6±0.2, 1.1±0.0, 1.3±0.1 and 1.4±0.2 (neurites/cell) for PC12 cells on PLL coated nanoprous SU-8 surface after 1, 3, 5 and 7 day's culture, respectively. At all the time points, the neurite numbers of PC12 cells is significantly greater on three types (Figure 4.7b, c, d) of surfaces relative to smooth bare (Figure 4.7a) SU-8 surface. Cells on PLL coated smooth (Figure 4.7b) and uncoated nanoporous (Figure 4.7c) SU-8 surface showed similar neurite numbers after 3, 5 and 7 days' culture, but the neurite numbers on PLL coated smooth (Figure 4.7b) SU-8 surface was slightly larger than uncoated nanoporous (Figure 4.7c) SU-8 surface. The neurite numbers on PLL coated nanoporous (Figure 4.7d) SU-8 surface were prone to increase gradually between 1 and 7 days.

Figure 4.8 shows the average neurite lengths of PC12 cells cultured on the four types of surface. Figure 4.8a shows that the average neurite lengths was 0.0 μm, 0.0 μm, 8.6±5.7 μm and 9.5±9.5 μm for PC12 cells on the smooth bare SU-8 surface after 1, 3, 5 and 7 days' culture, respectively. Figure 4.8b was 33.5±9.5 μm, 66.5±8.4 μm, 100.7±13.3 μm and 104.7±13.0 μm for PC12 cells on poly-L-lysine coated SU-8 surface after 1, 3, 5 and 7 days' culture, respectively. Figure 4.8c was 33.7±8.3 μm, 63.8±7.3 μm, 147.1±9.9 μm and 107.5±8.9 μm for PC12 cells on uncoated nanoprous SU-8 surface after 1, 3, 5 and 7 days' culture, respectively. Figure 4.8d was 18.7±6.0 μm, 49.1±5.2 μm, 106.4±8.2 μm and 146.4±26.4 μm for PC12 cells on PLL coated nanoprous SU-8 surface after 1, 3, 5 and 7 day's culture, respectively. At all the time points, the average neurite lengths of PC12 cells is significantly longer on three types (Figure 4.8b, c, d) of surfaces relative to smooth bare (Figure 4.8a) SU-8 surface. Cells on PLL coated smooth (Figure 4.8b) SU-8 surface after 5 days' culture showed almost maximal length of neurite that did not increase significantly for the remainder of the study, that is, after 7 days' culture. Cells on uncoated nanoporous (Figure 4.8c) SU-8 surface also showed maximal length of neurite after 5 days' culture, but the neurite length was decreased after 7 days' culture. Cells on PLL coated nanoporous (Figure 4.8d) SU-8 surface were prone to increase gradually between 1 and 7 days.
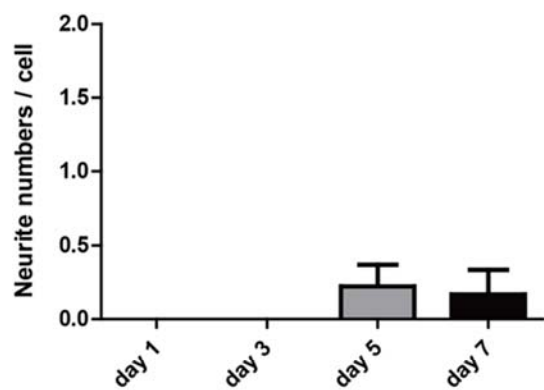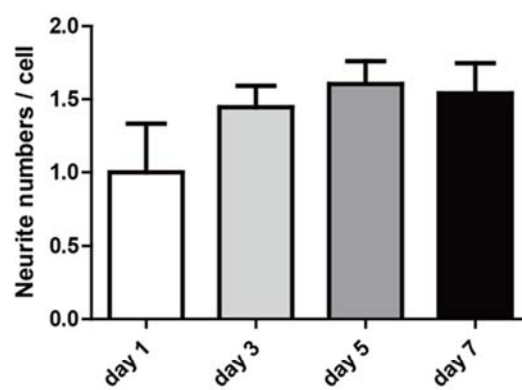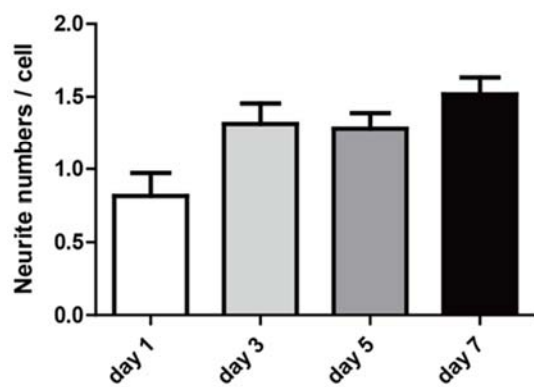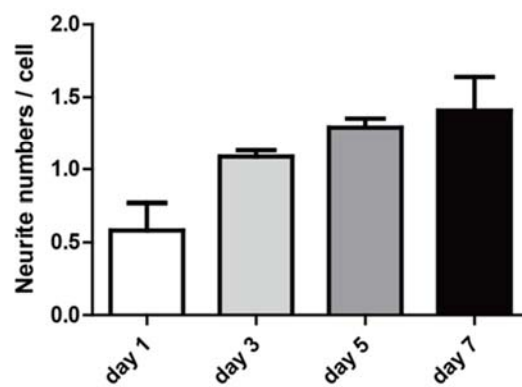
Figure 4.7   Bar graphs show the quantitative analysis of the neurites numbers per a PC12 cell on surfaces with different topography. Cells cultured on: (a) uncoated smooth bare; (b) poly-L-lysine coated smooth; (c) uncoated nanoporous; (d) poly-L-lysine coated nanoporous SU-8 surfaces. Values reported are mean ± standard error.
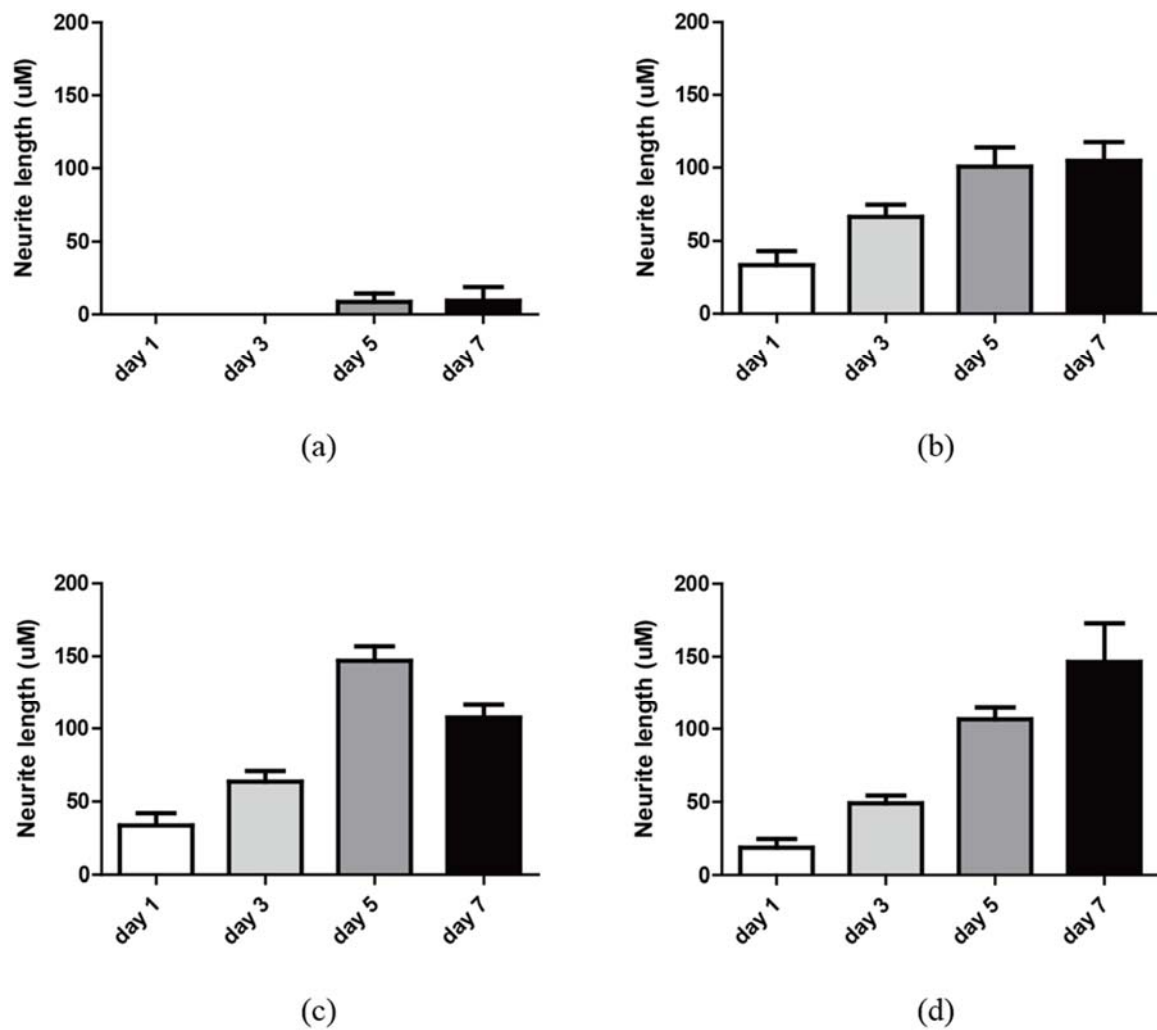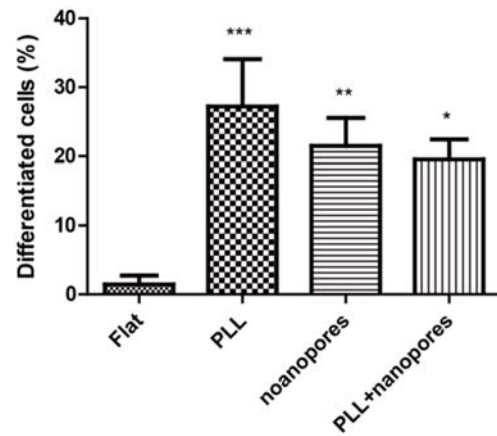
Figure 4.8 Bar graphs show the quantitative analysis of the neurite length on surfaces with different topography. Cells cultured on: (a) uncoated smooth bare; (b) poly-L-lysine coated smooth; (c) uncoated nanoporous; (d) poly-L-lysine coated nanoporous SU-8 surfaces. Values reported are mean ± standard error.

Figure 4.9 shows the differentiation level (Figure 4.9a, b), the neurite numbers per a PC12 cell (Figure 4.9c, d) and the average neurite length (Figure 4.9e, f). Comparisons were made on uncoated smooth bare, poly-L-lysine coated smooth, uncoated nanoporous and PLL coated nanoporous SU-8 surface after 5 days' (Figure 4.9a, c, e) and 7 days' (Figure 4.9b, d, f) culture. The differentiation level of PC12 cells cultured on uncoated nanoporous and PLL coated nanoporous SU-8 surface after 7 days' culture increased as long as the differentiation level after 5 days' culture on PLL coated smooth SU-8 surface. Likewise, the neurite numbers on PLL coated smooth SU-8 reached the maximal value after 5 days' culture, followed by uncoated nanoporous and PLL coated nanoporous SU-8 surface with the maximal neurite numbers after 7 days' culture. The average neurite length on uncoated nanoporous SU-8 surface showed the longest neurite after 5 days' culture. However, its average neurite length decreased after 7 days' culture. Cells on PLL coated nanoporous SU-8 surface after 7 days' culture showed the longest neurite length. The differentiation level, the neurite numbers and the average neurite length on three types of surfaces (PLL coated smooth, uncoated nanoporous and PLL coated nanoporous SU-8 surface) were significantly greater than those on uncoated smooth bare SU-8 surface after 5 and 7 days' culture (p < 0.001). Among three types of surfaces (PLL coated smooth, uncoated nanoporous and PLL coated nanoporous SU-8 surface) after 7 days' culture, there was no significant difference in differentiation level, neurite numbers and neurite length. In other words, nanoporous SU-8 surface without poly-L-lysine, a type of cell adhesive molecule, exhibited the effect as long as poly-L-lysine coating (PLL coated smooth SU-8 surface).

According to previous studies, the rate of differentiation and growth of cells on the different surfaces depend on the successful initial attachment of the cells on the surface of the substratum [33]. It was also reported that surface characteristics of materials such as wettability could influence nerve cell adhesion, and therefore

influence nerve cell differentiation and growth [34]. In this work, smooth bare SU-8 surface expected to have the highest contact angle and its surface charge is very poor, because this surface showed poor adhesion and growth of PC12 cells.

An understanding of nerve cell and biomaterial interactions *in vitro* should be the first important step in predicting the suitability of a biomaterial for nerve regeneration. The surface properties of biomaterials, including wettability and surface charge, may influence cellular responses to biomaterial implants [35]. Thus significant research efforts have focused on modifying surface physical and chemical properties to generate surfaces with better biocompatibility. In this work, we have shown that nerve cell development on nanoporous SU-8 surface without any cell adhesive molecules was as long as PLL coated smooth SU-8 surface implying that nanoporous SU-8 surface is a promising candidate surface for applying in biomedical field. However, further in vitro and in vivo studies are needed to analysis the interaction between nanoporous surface and cells and the function of filopodia as well as to evaluate the effect of this surface topography in promoting nerve regeneration.
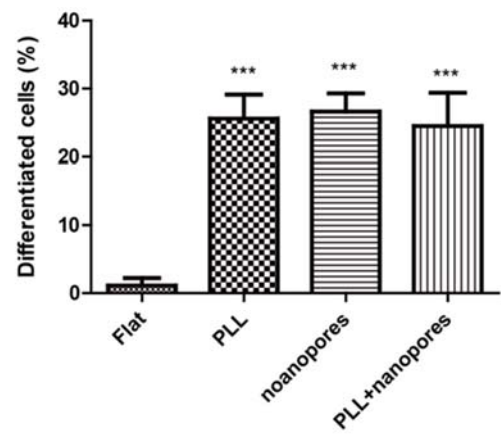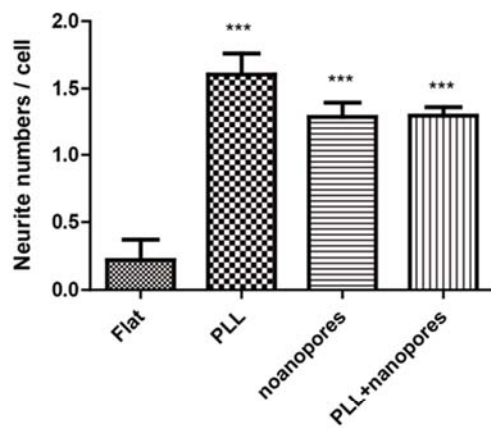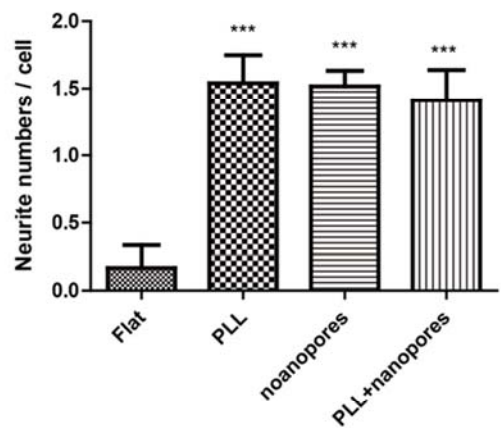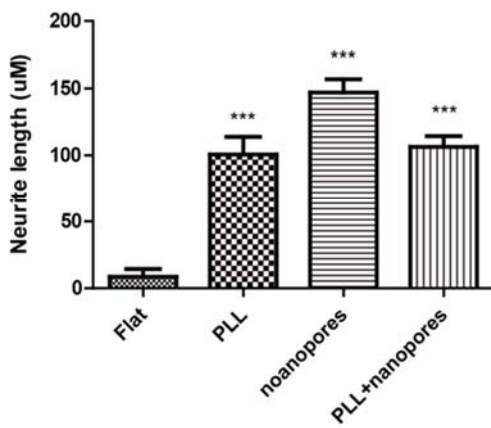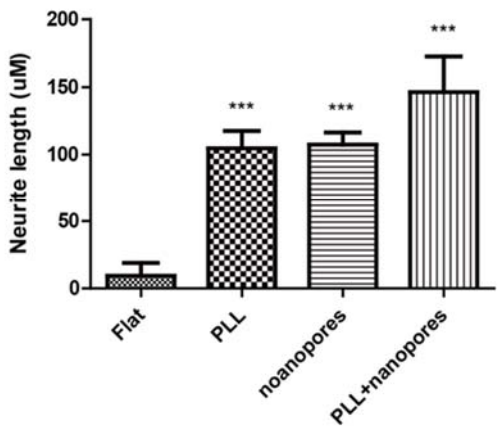
Figure 4.9 Bar graphs show the quantitative analysis of different cellular activities on surfaces with different topography. The mean: (a, b) differentiation level; (c, d) neurite numbers; (e, f) neurite length. The quantitative analysis after 5 days' culture (a, c, e) and after 7 days' culture (b, d, f). Values reported are mean ± standard error.

Characterizing Cell Morphology on Different Types of Surfaces. The cell morphology on four different types of surfaces was characterized by SEM. In Figure 4.10, after 7 days' culture four SEM images of PC12 cells cultured on uncoated smooth bare (a), poly-L-lysine coated smooth (b), uncoated nanoporous (c) and PLL coated nanoporous (d) SU-8 surface, respectively, are given. In each figure, only one cell body was selected that it can be visibly distinguish and has the longest neurite between different cell bodies. The size of selected cell bodies was about 20 ~ 25 μm (white ovals). The images in the dashed white boxes will be enlarged in Figure 4.11.

(a)   (b)

(c)   (d)
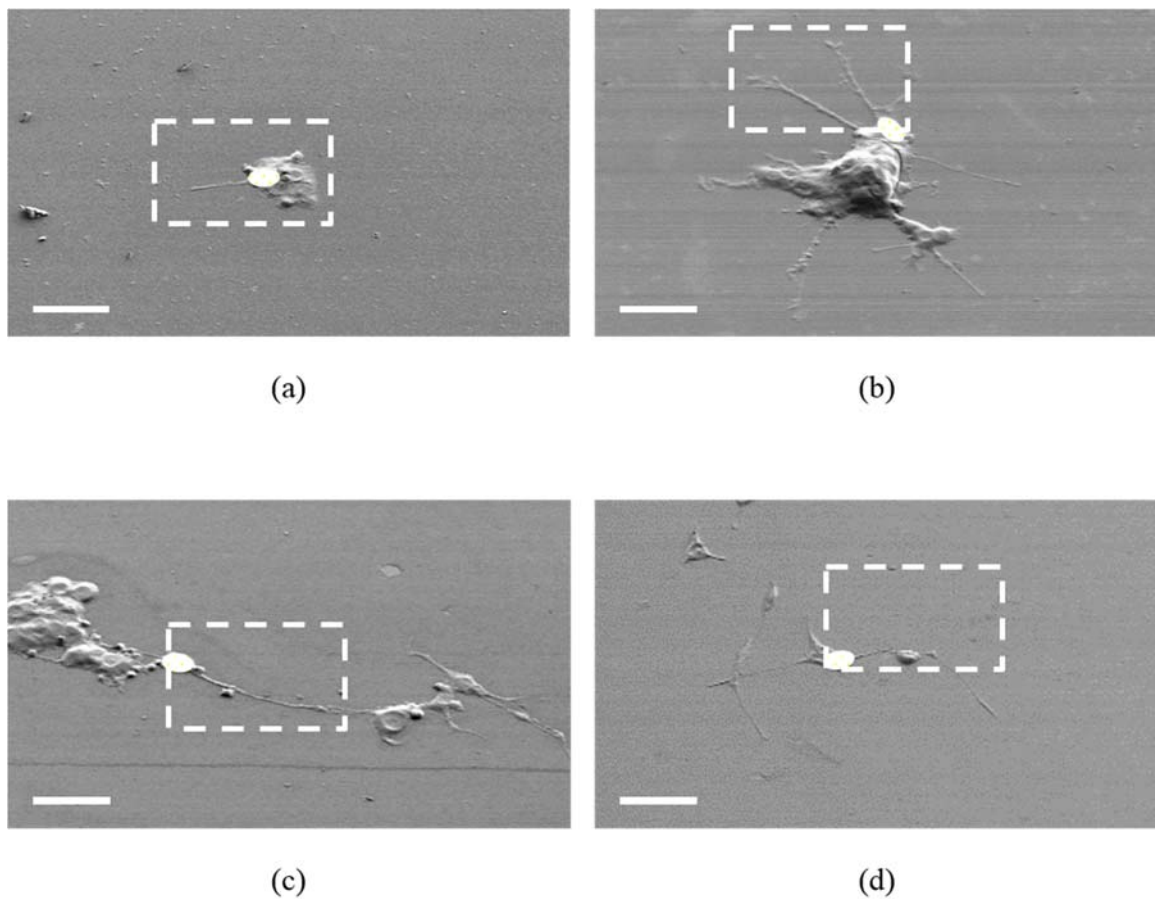
Figure 4.10   Scanning electron microscope (SEM) photographs of cells cultured on surfaces with different topography. Cells cultured on: (a) uncoated smooth bare; (b) poly-L-lysine coated smooth; (c) uncoated nanoporous; (d) poly-L-lysine coated nanoporous SU-8 surfaces. White ovals indicate the size of somas and it was about 20 to 25 μm. The images in the dashed white boxes will be enlarged in Figure 4.11. The scale bar represents 50 μm.

In Figure 4.11, four SEM image, at a mid-magnification, of cells on uncoated smooth bare, PLL coated smooth, uncoated nanoporous and PLL coated nanoprous SU-8 surfaces, respectively, are shown. Figure 4.11a shows cells cultured on uncoated smooth bare SU-8 surface with short and few neurites and neurite length of this surface was about 32 nm. Figure 4.11b and c show cells on PLL coated smooth and uncoated nanoporous SU-8 surface with intermediate length neurites, about 85 nm and 87 nm, respectively. Figure 4.11d shows cells cultured on PLL coated nanoporous SU-8 surface with long neurites, about 132 nm. The white arrows indicate the end of neurites that will be enlarged in Figure 4.12.

(a)　　　　　　　　　　　　　　(b)

(c)　　　　　　　　　　　　　　(d)
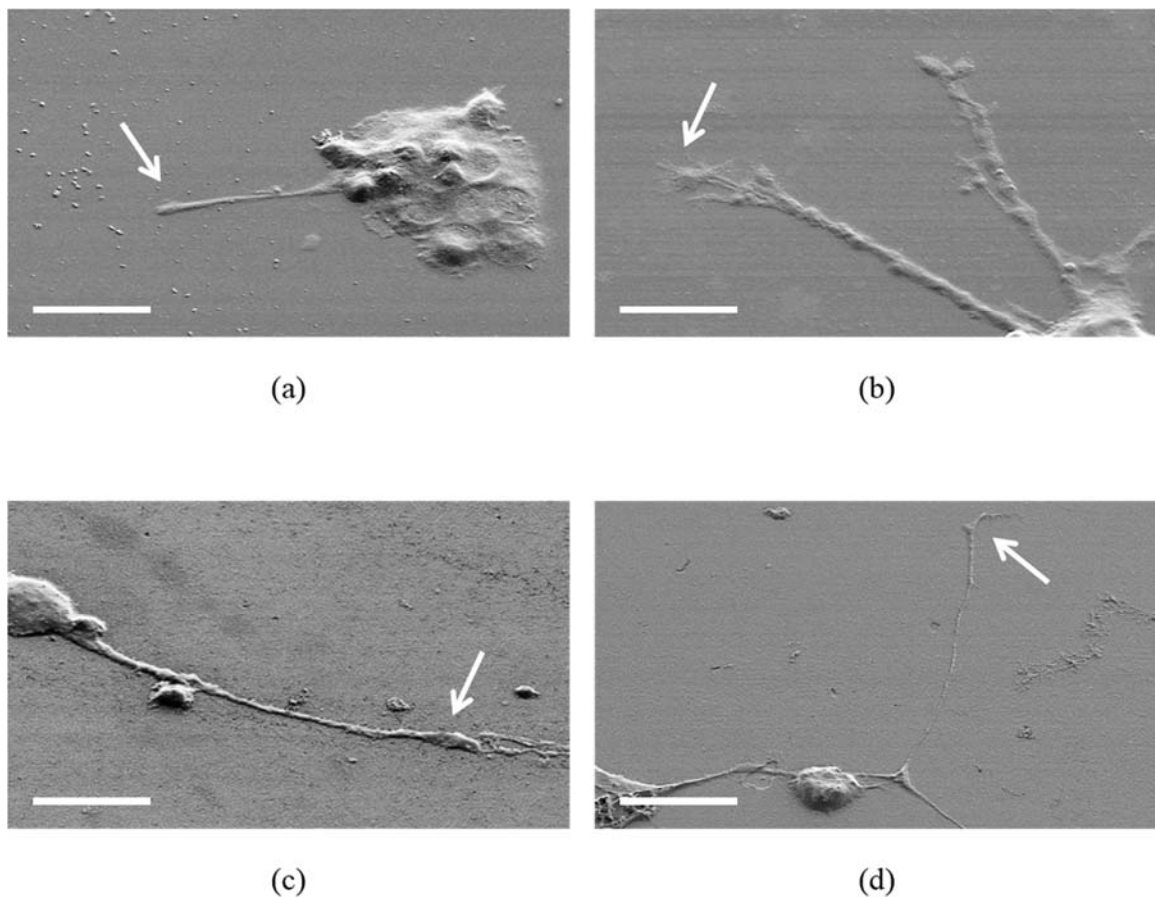
Figure 4.11　A mid-magnification SEM photographs of cells cultured on surfaces with different topography. Cell on: (a) uncoated smooth bare surface had a short neurite; (b) poly-L-lysine coated smooth surface had intermediate length neurites; (c) uncoated nanoporous surface had intermediate length neurites; (d) poly-L-lysine coated nanoporous surface had long neurites. The scale bar represents 25 μm.

The SEM of cells on different types of surfaces shows that the growth cone-like shape is different on four types of surfaces. Figure 4.12 shows four SEM images at a higher magnification, of cells on different types of surfaces. Figure 4.12a shows the end of neurite on uncoated smooth bare SU-8 surface with flat shape and it does not have filopodia. Figure 4.12b shows the end of neurite on PLL coated smooth SU-8 surface with flat shape and numerous filopodia. Figure 4.12c shows the end of neurite on uncoated nanoporous SU-8 surface with thick shape and unobserved filopodia. Figure 4.12d shows the end of neurite on PLL coated nanoporous SU-8 surface with thick but narrow shape and filopodia was not observed on this surface. These findings support our results in that the topography of nanoporous surface affects the growth cone-like shape. These differences in the growth cone-like shape could lead to different responses in neurite development [36].
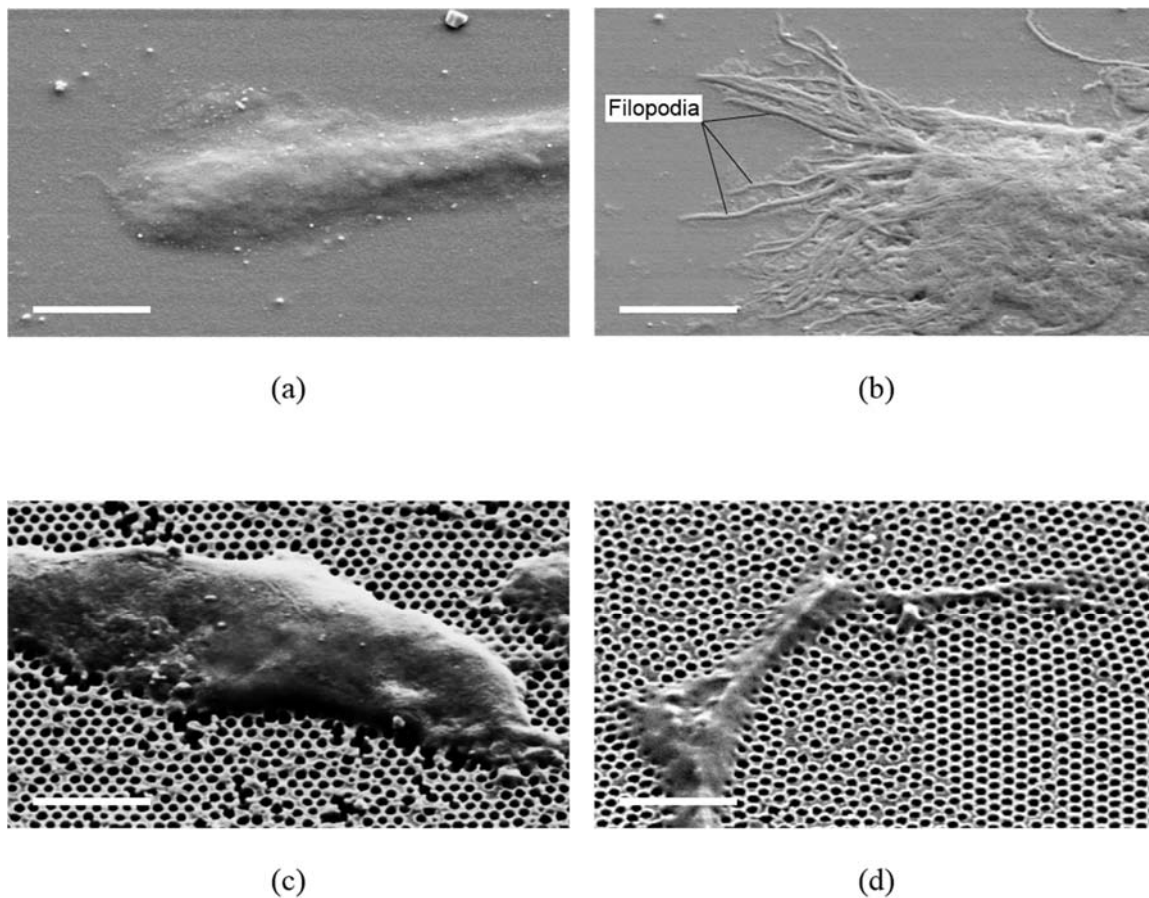
Figure 4.12 A higher magnification SEM photographs of cells cultured on surfaces with different topography. A neurite on: (a) uncoated smooth bare surface had flat groth cone-like shape; (b) poly-L-lysine coated smooth surface had flat and many filopodia on growth cone-like shape; (c) uncoated nanoporous surface had thick growth cone-like shape; (d) poly-L-lysine coated nanoporous surface had thick and narrow growth cone-like shape. The scale bar represents 2.5 μm.

5. CONCLUSIONS

5.1 Conclusions

This thesis has presented the effect of the nanoporous SU-8 surface on the in vitro neurite outgrowth of PC12 cells. The nano-pore arrays has been successfully fabricated on the SU-8 surface by using nanolithography technique. For quantitative analysis on neurite outgrowth, mainly three type of analysis have been performed and the results show that the nanoporous SU-8 surface has positive effect compared to the smooth SU-8 surface.

The thesis explains how to fabricate the nano-pore array on top of the SU-8 surface. To fabricate the nanopore arrays, we used polystyrene (PS) nanoparticles as a template of nanopore arrays. After etching the PS, chromium as a mask for etching the surface of SU-8 was deposited on top of PS particles and a vacant between PS particles. After removing PS particles and by etching the surface of SU-8, finally well-ordered nanopore arrays are created on the surface of SU-8.

Mainly three types of quantifications have been performed for analyzing neurite outgrowth in PC12 cells. First, the differentiation level means how many PC12 cells extended neurites like the morphology neural cells have. In smooth surface, cells were nearly not differentiated. However, after 7 days' culture, PLL coated smooth, nanoporous and PLL coated nanoporous surface had no significant difference. Second, the neurite numbers means how many neurites are in a PC12 cell. It can be described as neurite development. After 7 days' culture, the mean neurite numbers on smooth surface were very low than that on other surfaces. On the other hand, no obvious effect was found on PLL coated smooth, nanoporous and PLL coated nanoporous surfaces. Third, the neurite length also

means neurite development in PC12 cells but different results with the neurite numbers were founded. In smooth surface, cells show the shortest neurite length. In PLL coated nanoporous surface, cells had the longest neurite length than PLL coated smooth and nanoporous surfaces. Interestingly, for the results of neurite length during a week, PLL coated smooth surface had low neurite length compared to nanoporous and PLL coated nanoporous surface.

In conclusion, this thesis has shown the neurite development of PC12 cells on nanoporous SU-8 surface that are not coated with cell adhesion molecules like poly-L-lysine. This results is by far better than the smooth PLL-uncoated surface. Therefore, if this nanoporous surface is applied to the surface of implantable neural probe, we could expect the improved results as long-term neuronal recordings than the neural probe with smooth surface. That may because such bioactive surface (nanostructured porous SU-8) is able to allow for neuron to interact with electrode sites (recording sites) which have nano-scale features.

5.2 Future work

- Further *in vitro* and *in vivo* experimentation should be completed to analyze the activity of neurons in the surface with pores of various sizes.

- After the analysis of the pore sizes, actually metal electrode such as platinum or gold should be deposited on the surface of this nanoporous SU-8 to verify whether the neurite is induced into the electrode site.

- The assessment to the characterization of electrode, such as the impedance, should be employed to conform the improvement in the ability of SU-8 based nanoporous microelectrodes. In addition, if a lot of neurons on the electrode site will appear in the good quality of the signal.

References

[1] Y. Kato, I. Saito, T. Hoshino, T. Suzuki, and K. Mabuchi, "Preliminary study of multichannel flexible neural probes coated with hybrid biodegradable polymer," *Conf Proc IEEE Eng Med Biol Soc,* vol. 1, pp. 660-3, 2006.

[2] K. P. Das, T. M. Freudenrich, and W. R. Mundy, "Assessment of PC12 cell differentiation and neurite growth: a comparison of morphological and neurochemical measures," *Neurotoxicol Teratol,* vol. 26, pp. 397-406, May-Jun 2004.

[3] K. Frank and M. C. Becker, "Microelectrodes for recording and stimulation," *Physical techniques in biological research,* vol. 5, pp. 22-87, 1964.

[4] M. A. Nicolelis and M. A. Lebedev, "Principles of neural ensemble physiology underlying the operation of brain–machine interfaces," *Nature Reviews Neuroscience,* vol. 10, pp. 530-540, 2009.

[5] K. D. Wise, "Silicon microsystems for neuroscience and neural prostheses," *Engineering in Medicine and Biology Magazine, IEEE,* vol. 24, pp. 22-29, 2005.

[6] T. D. Y. Kozai and D. R. Kipke, "Insertion shuttle with carboxyl terminated self-assembled monolayer coatings for implanting flexible polymer neural probes in the brain," *Journal of neuroscience methods,* vol. 184, pp. 199-205, 2009.

[7] R. A. Normann, "Technology insight: future neuroprosthetic therapies for disorders of the nervous system," *Nature Clinical Practice Neurology,* vol. 3, pp. 444-452, 2007.

[8] J. P. Seymour and D. R. Kipke, "Neural probe design for reduced tissue encapsulation in CNS," *Biomaterials,* vol. 28, pp. 3594-3607, 2007.

[9] M. NEVAS, "Advances in cerebral probing using modular multifunctional probe arrays," *Medical device technology,* vol. 18, pp. 38-39, 2007.

[10] K. E. Jones, P. K. Campbell, and R. A. Normann, "A glass/silicon composite intracortical electrode array," *Annals of biomedical engineering,* vol. 20, pp. 423-437, 1992.

[11] C. Xu, W. Lemon, and C. Liu, "Design and fabrication of a high-density metal microelectrode array for neural recording," *Sensors and Actuators A: Physical,* vol. 96, pp. 78-85, 2002.

[12] M. Tijero, G. Gabriel, J. Caro, A. Altuna, R. Hernández, R. Villa, *et al.*, "SU-8 microprobe with microelectrodes for monitoring electrical impedance in living tissues," *Biosensors and Bioelectronics,* vol. 24, pp. 2410-2416, 4/15/ 2009.

[13] M. Eddleston and L. Mucke, "Molecular profile of reactive astrocytes—implications for their role in neurologic disease," *Neuroscience,* vol. 54, pp. 15-36, 1993.

[14] V. S. Polikov, P. A. Tresco, and W. M. Reichert, "Response of brain tissue to chronically implanted neural electrodes," *Journal of neuroscience methods,* vol. 148, pp. 1-18, 2005.

[15] Y.-T. Kim, R. W. Hitchcock, M. J. Bridge, and P. A. Tresco, "Chronic response of adult rat brain tissue to implants anchored to the skull," *Biomaterials,* vol. 25, pp. 2229-2237, 2004.

[16] A. B. Schwartz, X. T. Cui, Douglas J. Weber, and D. W. Moran, "Brain-Controlled Interfaces: Movement Restoration with Neural Prosthetics," *Neuron,* vol. 52, pp. 205-220, 10/5/ 2006.

[17] S. Retterer, K. Smith, C. Bjornsson, J. Turner, M. Isaacson, and W. Shain, "Constant pressure fluid infusion into rat neocortex from implantable microfluidic devices," *Journal of Neural Engineering,* vol. 5, p. 385, 2008.

[18] Y. Zhong and R. V. Bellamkonda, "Dexamethasone-coated neural probes elicit attenuated inflammatory response and neuronal loss compared to uncoated neural probes," *Brain research,* vol. 1148, pp. 15-27, 2007.

[19] Y. Xiao, D. C. Martin, X. Cui, and M. Shenai, "Surface modification of neural probes with conducting polymer poly (hydroxymethylated-3, 4-ethylenedioxythiophene) and its biocompatibility," *Applied Biochemistry and Biotechnology,* vol. 128, pp. 117-129, 2006.

[20] J. L. McKenzie, M. C. Waid, R. Shi, and T. J. Webster, "Decreased functions of astrocytes on carbon nanofiber materials," *Biomaterials,* vol. 25, pp. 1309-1317, 2004.

[21] K. A. Moxon, N. M. Kalkhoran, M. Markert, M. A. Sambito, J. McKenzie, and J. T. Webster, "Nanostructured surface modification of ceramic-based microelectrodes to enhance biocompatibility for a direct brain-machine interface," *Biomedical Engineering, IEEE Transactions on,* vol. 51, pp. 881-889, 2004.

[22] Y. Xia, B. Gates, Y. Yin, and Y. Lu, "Monodispersed Colloidal Spheres: Old Materials with New Applications," *Advanced Materials,* vol. 12, pp. 693-713, 2000.

[23] J. C. Hulteen and R. P. Van Duyne, "Nanosphere lithography: A materials general fabrication process for periodic particle array surfaces," *Journal of Vacuum Science & Technology A: Vacuum, Surfaces, and Films,* vol. 13, pp. 1553-1558, 05/00/ 1995.

[24] N. Marquestaut, A. Martin, D. Talaga, L. Servant, S. Ravaine, S. p. Reculusa*, et al.*, "Raman Enhancement of Azobenzene Monolayers on Substrates Prepared by Langmuir−Blodgett Deposition and Electron-Beam Lithography Techniques," *Langmuir,* vol. 24, pp. 11313-11321, 2008/10/07 2008.

[25] D. Qiu, T. Cosgrove, P. Revell, and I. Howell, "Poly(ethylene oxide) Adsorption on Polystyrene Latex Particles in the Presence of Poly(styrenesulfonate sodium)," *Macromolecules,* vol. 42, pp. 547-552, 2009/01/27 2008.

[26] J. W. Yang, J. I. Sim, H. M. An, and T. G. Kim, "Fabrication of nanometer-scale pillar structures by using nanosphere lithography," *J. Korean Phys. Soc,* vol. 58, pp. 994-997, 2011.

[27] C. Lyman, D. Newbury, J. Goldstein, D. Williams, A. Romig, and J. Armstrong, "Scanning electron microscopy, X-ray microanalysis and analytical electron microscopy," *Plenum Press: New York. $29.25 (pb). Review by I. Brough in: J. Microsc,* vol. 164, p. 179, 1991.

[28] A. Bershadsky, A. Chausovsky, E. Becker, A. Lyubimova, and B. Geiger, "Involvement of microtubules in the control of adhesion-dependent signal transduction," *Current Biology,* vol. 6, pp. 1279-1289, 1996.

[29] A. Krause, E. A. Cowles, and G. Gronowicz, "Integrin-mediated signaling in osteoblasts on titanium implant materials," *Journal of biomedical materials research,* vol. 52, pp. 738-747, 2000.

[30] D. Mazia, G. Schatten, and W. Sale, "Adhesion of cells to surfaces coated with polylysine. Applications to electron microscopy," *The Journal of cell biology,* vol. 66, pp. 198-200, 1975.

[31] G. Rainaldi, P. Filippini, A. Ferrante, P. L. Indovina, and M. T. Santini, "Fibronectin facilitates adhesion of K562 leukemic cells normally growing in suspension to cationic surfaces," *Journal of biomedical materials research,* vol. 55, pp. 104-113, 2001.

[32] L. A. Greene, M. Sobeih, and K. Teng, "Methodologies for the culture and experimental use of the PC12 rat pheochromocytoma cell line," *Culturing nerve cells,* pp. 207-226, 1991.

[33] A. El-Ghannam, P. Ducheyne, and I. M. Shapiro, "Bioactive material template for in vitro, synthesis of bone," *Journal of biomedical materials research,* vol. 29, pp. 359-370, 1995.

[34] S. J. Lee, G. Khang, Y. M. Lee, and H. B. Lee, "The effect of surface wettability on induction and growth of neurites from the PC-12 cell on a polymer surface," *Journal of colloid and interface science,* vol. 259, pp. 228-235, 2003.

[35] J. H. Lee, H. W. Jung, I.-K. Kang, and H. B. Lee, "Cell behaviour on polymer surfaces with different functional groups," *Biomaterials,* vol. 15, pp. 705-711, 1994.

[36] P. Clark, S. Britland, and P. Connolly, "Growth cone guidance and neuron morphology on micropatterned laminin surfaces," *Journal of cell science,* vol. 105, pp. 203-212, 1993.

요 약 문

뇌-기계 간 인터페이스(BMI)의 기능을 향상시키기 위한
SU-8 기반 나노 다공성 표면의 제작

본 논문은 신경 세포의 신경돌기(neurite)의 성장을 향상시키기 위한 신경전극의 표면처리 방법으로 나노 크기의 다공성 구조를 SU-8 의 표면에 제작하는 방법을 제안한다.

신경전극은 손상된 운동기관이나 감각기관의 신경을 회복하기 위한 뇌-기계 인터페이스(BMI)를 위해 필요한 장치로써 이와 관련된 많은 연구들이 진행되어 왔다. 인공 와우(artificial coclear), 신경 보철 전극과 같은 인체 삽입형 전극은 외부로부터의 자극을 뇌로 전달하거나, 신경 세포로부터 신호를 받아 인공 팔이나 인공 다리와 같은 외부 장치를 움직이게 하는 신호 전달 매개체로써 중요한 역할을 한다. 신경 세포로부터 신경 신호를 기록하는데 있어서 가장 문제가 되는 것은 신경전극이 신경조직에 삽입되면 면역반응에 의해 염증이 일어나게 되고, 그 부위를 신경교세포(neuroglia)가 둘러 쌓으면서 신경교성반흔(glia-scar)이 생기는 것이다. 이러한 신경 교성반흔은 신경세포가 전극의 기록 부위에 접근하는 것을 차단시키기 때문에 삽입된 신경 전극이 신경 세포로부터 신호를 받는 것을 방해하게 된다. 따라서 전극에서 신경 세포로부터 지속적으로 전기신호를 얻기 위해서는 신경교세포(neuroglia) 보다는 신경 세포(neuron)와 상호 작용을 향상시킬 수 있는 표면이 필요하다.

또한 신경조직은 많은 나노 크기의 세포 외 미세소관(extracellular microtubules)과 라미닌 (laminin)과 같은 단백질로 이루어져 있기 때문에 신경세포는 나노 크기의 표면과 상호작용할 것이다. 이러한 신경세포와의 결합을 향상시키기 위해 화학적인 방법으로 표면을 처리하는 연구가 개발되어왔다. 그러나 이러한 화학적인 표면처리는 장기간 동안 그 기능이 유지되기 어렵다. 따라서 장기간 동안 신경 전극의 효율성을 유지하기 위해서 전극의 표면이 물리적인 구조를 가지는 것이 선호된다.

따라서 본 논문에서는 유연한 폴리머 신경 전극으로 주로 이용되는 SU-8 을 전극의 기반이 될 것으로 가정하고, 나노 구 리소그래피(NSL; Nanosphere Lithography) 방법으로 폴리 스타이렌(polystyrene)을 마스크로 이용하여 약 200 nm 크기의 나노 다공성 구조를 가진 SU-8 표면을 제작하였다. 또한, 제작된 나노 다공성의 SU-8 표면과 평평한 SU-8 의 표면에서 신경 세포 연구를 위한 모델 세포로 주로 이용되는 PC12 세포를 분화시켜 표면의 형상에 대해 어떤 차이가 있는지 실험을 통하여 증명한다.

핵심어: 나노 다공성, 표면 처리, 뇌-기계 인터페이스 기술(BMI), 나노 구 리소그래피(NSL)

Acknowledgement